Vibrational (resonance) Raman optical activity with real time time dependent density functional theory

Mattiat, Johann ; Luber, Sandra

Abstract: We present a novel approach for the calculation of vibrational (resonance) Raman optical activity (ROA) spectra based on real time propagation. The ROA linear electronic response tensors are formulated in a propagator formalism in order to treat linear response (LR-) and real time time dependent density functional theory (RT-TDDFT) on equal footing. The length, mixed, and velocity representations of these tensors are discussed with respect to the potential origin dependence of the ROA invariants in the calculations. The propagator formalism allows a straight forward extension of the optical LR tensors in a mixed or velocity representation to a coupling with nonlocal potentials, where an extra term appears in the definition of the momentum operator, in order to maintain the gauge invariance. Using RT-TDDFT paves the way for an innovative, efficient calculation of both on- and off-resonance ROA spectra. Exemplary results are given for the off-resonance and (pre-)resonance spectra of (R)-methyloxirane, considering the resonance effects due to one or more electronically excited states. Moreover, the developed real time propagation approach allows us to obtain entire excitation profiles in a computationally efficient way.

DOI: https://doi.org/10.1063/1.5132294

The Journal of Chemical Physics

Vibrational (resonance) Raman optical activity with real time time dependent density functional theory

Cite as: J. Chem. Phys. **151**, 234110 (2019); https://doi.org/10.1063/1.5132294@jcp.2019.EISC2019.issue-1
Submitted: 16 October 2019 . Accepted: 29 November 2019 . Published Online: 18 December 2019

Johann Mattiat, and Sandra Luber

The Journal of Chemical Physics ARTICLE scitation.org/journal/jcp

Vibrational (resonance) Raman optical activity with real time time dependent density functional theory

Cite as: J. Chem. Phys. 151, 234110 (2019); doi: 10.1063/1.5132294
Submitted: 16 October 2019 • Accepted: 29 November 2019 •
Published Online: 18 December 2019

Johann Mattiat and Sandra Luber[a)]

AFFILIATIONS

Department of Chemistry, University of Zurich, Zurich, Switzerland

Note: This paper is part of the JCP Emerging Investigators Special Collection.
[a)]**Electronic mail:** sandra.luber@chem.uzh.ch

ABSTRACT

We present a novel approach for the calculation of vibrational (resonance) Raman optical activity (ROA) spectra based on real time propagation. The ROA linear electronic response tensors are formulated in a propagator formalism in order to treat linear response (LR-) and real time time dependent density functional theory (RT-TDDFT) on equal footing. The length, mixed, and velocity representations of these tensors are discussed with respect to the potential origin dependence of the ROA invariants in the calculations. The propagator formalism allows a straight forward extension of the optical LR tensors in a mixed or velocity representation to a coupling with nonlocal potentials, where an extra term appears in the definition of the momentum operator, in order to maintain the gauge invariance. Using RT-TDDFT paves the way for an innovative, efficient calculation of both on- and off-resonance ROA spectra. Exemplary results are given for the off-resonance and (pre-)resonance spectra of (R)-methyloxirane, considering the resonance effects due to one or more electronically excited states. Moreover, the developed real time propagation approach allows us to obtain entire excitation profiles in a computationally efficient way.

I. INTRODUCTION

Vibrational Raman Optical Activity (ROA) has become an invaluable tool in order to obtain structural information about systems ranging from small molecules to proteins and even viruses,[1] making use out of its sensitivity to chirality. The experimental technique has been applied to determine absolute configurations,[2,3] the study of chiral ionic liquids,[4] the observation of biomolecules in solutions,[5,6] the study of paramagnetic molecules[7] and the deep UV region[8] for the investigation of the preresonant and resonant Raman and ROA scattering.

The broad applicability of Raman and ROA spectroscopy for the investigation of a variety of systems calls for theoretical modeling with the aim of a better interpretation of these experiments. With a general theory and experimental techniques for ROA developed already in the 1960s and 1970s,[9–13] one of the main obstacles for accurate modeling of (resonance) ROA spectra is still the huge dimensionality of the problem, since not only the electronic but also the vibrational states need to be described.

The calculation of ROA spectra in the nonresonant regime has appeared at the end of the 1980s[14] and since then has been performed on a variety of systems. After the first calculations at a Hartree–Fock level of theory,[15,16] many density functional theory (DFT)[17–24] and later higher level of theory studies[25,26] followed. Advances for speeding up the calculations include the calculation of analytical ROA intensity differences,[27] density fitting,[28] Cartesian transfer,[29] molecules in molecules fragmentation schemes,[30] and intensity tracking.[31] Moreover, the first entirely *ab initio* molecular dynamics based approach was presented recently[32] and the solvation and environmental effects were studied, including the polarizable continuum models[33–37] combined with molecular dynamics.[38–42] The first calculations for transition metal complexes[19,28,43–45] have also paved the way for experimental and computational studies (see Ref. 46 for the first review of ROA for transition metal containing

complexes and solids). For general reviews about the simulation of ROA spectra, see Refs. 6 and 47–50.

In the resonance regime, other approximations to the full vibronic response tensor have to be considered and in practical calculations further approximations have to be made. Mainly two methods have been developed for a resonant description of Raman (and ROA) spectra: the *vibronic theory* building on a formulation of Albrecht[51,52] and a family of *short time approximations* (STAs) mostly developed in the 1980s by Heller *et al.*[53–55] as part of their description of Raman scattering in the time domain. The vibronic theory, as well as approaches based on the time-dependent formulation, have later been adapted in a linear response time dependent density functional theory (LR-TDDFT) framework for the calculation of ROA spectra. These efforts include vibronic details in a gradient Franck–Condon model,[56] and Herzberg–Teller and Duschinsky effects,[57–59] or a Placzek type approximation.[60,61] Also, there is a recent expansion to X-ray ROA.[62]

Apart from the necessity to model both electronic and vibrational states, the sheer size of systems of experimental interest also hinders a large scale modeling of ROA spectra, which calls for efficient methods. A promising candidate is real time TDDFT (RT-TDDFT) that combines the advantages of DFT with a favorable scaling compared to LR-TDDFT.[63] The description of the dynamics in the time domain allows us to obtain all excited states from just one simulation run, without losing information about the individual transitions,[64] and works well also for a high density of states, which was demonstrated for a (resonance) Raman excitation profile.[65] Aside from that, pseudopotentials[66,67] may be used in order to describe chemically inert core electrons, which again reduces the computational resources needed for the calculation of ROA spectra and was recently implemented in CP2K[68–70] using density functional perturbation theory (DFPT) for static and dynamic[32] ROA calculations as well as their analysis in terms of localized molecular orbitals.[71]

A well known issue connected with the description of electromagnetic response properties such as electronic circular dichroism (ECD) and ROA is that calculations of the response properties show a dependence on the choice of the coordinate system, due to the inevitably finite basis sets in practical calculations.[72] In order to overcome this problem, mainly two methods have been developed: the use of gauge including atomic orbitals (GIAOs)[73–77] or a description of the magnetic response in the velocity representation.[28,32,60,78] The general idea behind these two approaches is to choose the gauge in a way such that the effects of the finite basis set are minimized. Both methods allow for origin independent results.

In this work, we will focus on the STA of the vibrational dynamics in an RT-TDDFT framework. We will reformulate the optical linear response tensors necessary for the calculation of ROA spectra in a propagator formalism of linear response in order to have a common framework applicable to both LR- and RT-TDDFT in addition to giving an intuitive perspective on the real time propagation (RTP) approaches to the linear response. In this formulation, different representations of the response tensors arise naturally and the origin dependence of the invariants of the response tensors can be discussed in a consistent and systematic fashion.

Another complexity that is covered naturally in the propagator formulation is a description of the coupling of nonlocal pseudopotentials to electromagnetic fields, where the operators have to be transformed consistently to their pseudopotential representation.[79–82] It can be shown that this transformation is necessarily gauge dependent. In practice, this leads to the introduction of the so called *generalized momentum* instead of the canonical momentum.[82,83]

The focus of this work is on the theoretical description of our approach. Calculations are presented for (R)-methyloxirane. However, the approach is rather general so that the available computational resources are mainly the limiting factor in large scale applications.

II. THEORY

The calculation of ROA spectra depends in general on five linear response tensors, the electric-dipole–electric-dipole polarizability $\boldsymbol{\alpha}$, the electric-dipole–magnetic-dipole polarizability $\boldsymbol{G}$, the magnetic-dipole–electric-dipole polarizability $\mathscr{G}$, the electric-dipole–electric-quadrupole polarizability $\boldsymbol{A}$, and the electric-quadrupole–electric-dipole polarizability $\mathscr{A}$, which may be considered as first order terms in a multipole expansion of the electric dipole moment, magnetic dipole moment, and electric quadrupole moment, respectively, with respect to an external electromagnetic field perturbation.[84–86] The spectra are then given in terms of various isotropic and anisotropic invariants of these generally complex valued response tensors, depending on the experimental setup, i.e., the direction and polarization of the perturbing field with respect to the orientation of the molecules (the rotational degrees of freedom are averaged out). To first order in the electric field E_β, the multipole expansions of the induced electric dipole moment d_α, the induced magnetic dipole moment m_α, and the induced electric quadrupole moment θ_α are given by[85]

$$d_\alpha = \left(\alpha_{\alpha\beta} + \frac{i\omega}{3c} n^i_\gamma A_{\alpha,\gamma\beta} + \frac{1}{c}\epsilon_{\gamma\delta\beta} n^i_\delta G_{\alpha\gamma} + \cdots\right) E_\beta, \tag{1}$$

$$m_\alpha = \left(\mathscr{G}_{\alpha\beta} + \cdots\right) E_\beta, \tag{2}$$

$$\theta_{\alpha\beta} = \left(\mathscr{A}_{\gamma,\alpha\beta} + \cdots\right) E_\gamma. \tag{3}$$

Greek indices denote the Cartesian room directions and the Einstein summation convention is used. n^i_γ denotes the propagation vector of the incident wave. The difference between the script tensors $\mathscr{G}_{\alpha\beta}$, $\mathscr{A}_{\gamma,\alpha\beta}$ and the Roman tensors $G_{\alpha\gamma}$, $A_{\alpha,\gamma\beta}$ is discussed in Refs. 85–87. The following discussion of the theory will focus on the Roman tensors.

Expressions for the response tensors are usually derived within perturbation theory, such as the well known Kramers–Heisenberg–Dirac (KHD) tensor, giving the electric-dipole–electric-dipole polarizability components,[88]

$$\alpha^{\mathrm{KHD}}_{\alpha\beta}(\omega_S) = -\sum_{k,v} \frac{\left\langle \chi^{0v''} \middle| a^{0k}_\alpha \middle| \chi^{kv} \right\rangle \left\langle \chi^{kv} \middle| a^{k0}_\beta \middle| \chi^{0v'} \right\rangle}{\hbar\omega_I - (E^v_k - E^{v'}_0) + i\hbar\Gamma} + \frac{\left\langle \chi^{0v''} \middle| a^{0k}_\beta \middle| \chi^{kv} \right\rangle \left\langle \chi^{kv} \middle| a^{k0}_\alpha \middle| \chi^{0v'} \right\rangle}{-\hbar\omega_S - (E^v_k - E^{v'}_0) + i\hbar\Gamma}, \tag{4}$$

given here in the Born–Oppenheimer approximation for a scattering event from the initial vibrational state v' of the electronic

ground state 0, $\left|\chi^{0v'}\right\rangle$, to the final vibrational state v'' of the electronic ground state 0, $\left|\chi^{0v''}\right\rangle$ (the vibrational index v runs over all the vibrational states within each electronic state k). $1/\Gamma$ corresponds to an averaged finite lifetime of the excited states, and E_k^v denotes the energy of the vth vibrational state on the kth Born-Oppenheimer surface. ω_I and ω_S are the angular frequencies of the incoming and the scattered light, respectively. The electronic transition dipole moment between the electronic ground state $|0\rangle$ and an electronically excited state $|k\rangle$ is given by

$$d_\alpha^{0k} = \langle 0|\hat{d}_\alpha|k\rangle, \tag{5}$$

where $\hat{d}_\alpha = -e\hat{r}_\alpha$ is the electric dipole moment operator for the electrons with e denoting the elementary charge and $\hat{r}_\alpha$ is the position operator.

Expressions for the electric-dipole–magnetic-dipole polarizability and the electric-dipole–electric-quadrupole polarizability are analogous with one of the electric dipole transition moment replaced either by the magnetic dipole transition moments $m_\beta^{k0} = \langle k|\hat{m}_\beta|0\rangle$ with the magnetic dipole moment operator,

$$\hat{m}_\beta = -\frac{e}{2m_e}\epsilon_{\beta\gamma\delta}\hat{r}_\gamma\hat{p}_\delta, \tag{6}$$

where m_e is the electron rest mass, $\hat{p}_\gamma$ is the momentum operator, and $\epsilon_{\alpha\beta\gamma}$ is the Levi–Civita tensor in three dimensions, or the electric quadrupole transition moments $\theta_{\beta\gamma}^{k0} = \langle k|\hat{\theta}_{\beta\gamma}|0\rangle$ with the (traceless) electric quadrupole moment operator,

$$\hat{\theta}_{\beta\gamma} = -\frac{e}{2}\left(3\hat{r}_\beta\hat{r}_\gamma - \delta_{\beta\gamma}\hat{r}_\alpha\hat{r}_\alpha\right). \tag{7}$$

A. Short time approximation

The direct calculation of these sum over states expressions is very demanding since all electronic and vibrational states have to be known beforehand. A common approximation is to replace the full expression given in Eq. (4) by a Taylor expansion in terms of normal mode coordinates q around the equilibrium geometry q_0,[89]

$$\alpha_{\alpha\beta}(\omega, q) = \alpha_{\alpha\beta}(\omega, q_0) + \sum_k \frac{\partial\alpha_{\alpha\beta}}{\partial q_k}\Big|_{q=q_0}(q_k - q_k^0) + \cdots, \tag{8}$$

where ω is the angular frequency and $\alpha_{\alpha\beta}(\omega, q)$ is an approximation of the electric-dipole–electric dipole polarizability, treating the vibrational degrees of freedom in terms of a normal mode expansion. A detailed derivation of this approach is spelled out in Ref. 90.

In the harmonic approximation, the 0th order term in Eq. (8) relates to the Rayleigh scattering and the 1st order term to the Raman scattering. If there is a clear separation of energy scales between the vibrational, photon, and electronic degrees of freedom, $\alpha_{\alpha\beta}(\omega, q)$ may be replaced by the real valued Placzek polarizability components,[91]

$$\alpha_{\alpha\beta}^{\text{Placzek}}(\omega, q) = \sum_k\left[\frac{d_\alpha^{0k}d_\beta^{k0}}{E_k(q) - E_0(q) - \hbar\omega} + \frac{d_\beta^{0k}d_\alpha^{k0}}{E_k(q) - E_0(q) + \hbar\omega}\right]. \tag{9}$$

Here, $E_k(q)$ is the energy of the kth BO surface at geometry q. Again, this line of reasoning is also valid for the linear response tensors $\boldsymbol{G}$ and $\boldsymbol{A}$ necessary for the ROA calculations.[10]

As shown by Lee[89] using the time domain representation of the KHD tensor,[53] this treatment can also be extended to the resonance case by using various semiclassical propagation schemes, as long as only the short time dynamics on the excited electronic potential energy surfaces are important. Consequently, this class of approximation is known as STAs. This Placzek type extension to the resonance case has been derived within a LR-TDDFT framework for the calculation of Raman[90,92] and ROA spectra[60] and works essentially by including the finite averaged lifetime of the electronic states $1/\Gamma$,

$$\alpha_{\alpha\beta}^{\text{el}}(\omega, q) = -\sum_k\left[\frac{d_\alpha^{0k}d_\beta^{k0}}{\hbar\omega - (E_k(q) - E_0(q)) + i\hbar\Gamma} + \frac{d_\beta^{0k}d_\alpha^{k0}}{-\hbar\omega - (E_k(q) - E_0(q)) + i\hbar\Gamma}\right], \tag{10}$$

$$G_{\alpha\beta}^{\text{el}}(\omega, q) = -\sum_k\left[\frac{d_\alpha^{0k}m_\beta^{k0}}{\hbar\omega - (E_k(q) - E_0(q)) + i\hbar\Gamma} + \frac{m_\beta^{0k}d_\alpha^{k0}}{-\hbar\omega - (E_k(q) - E_0(q)) + i\hbar\Gamma}\right], \tag{11}$$

$$A_{\alpha,\beta\gamma}^{\text{el}}(\omega, q) = -\sum_k\left[\frac{d_\alpha^{0k}\theta_{\beta\gamma}^{k0}}{\hbar\omega - (E_k(q) - E_0(q)) + i\hbar\Gamma} + \frac{\theta_{\beta\gamma}^{0k}d_\alpha^{k0}}{-\hbar\omega - (E_k(q) - E_0(q)) + i\hbar\Gamma}\right]. \tag{12}$$

It is also applicable within a RT-TDDFT framework for the calculation of Raman spectra[65,93] giving identical results as the LR-TDDFT approach for a weak perturbation.

The Raman and ROA intensities for each normal mode p within these STAs and the harmonic approximation are then given by

$$I_p = P_p S_p, \tag{13}$$

where P_p is a prefactor,[94]

$$P_p = \frac{\pi^2}{\epsilon_0}(\tilde{\nu}_{in} - \tilde{\nu}_p)^4\frac{h}{8\pi^2 c\tilde{\nu}_p}\frac{1}{1 - \exp[-hc\tilde{\nu}_p/k_BT]}, \tag{14}$$

with ϵ_0 being the permittivity of vacuum, c being the speed of light, $\tilde{\nu}_{in}$ and $\tilde{\nu}_p$ being the wavenumbers of the incoming photon and the normal mode p, respectively, k_B being the Boltzmann constant, and T being the temperature. The scattering factor S_p depends on the kind of spectroscopy (Raman or ROA) and the experimental setup and contains the invariants[87]

$$\boldsymbol{\alpha}^2 = \frac{1}{9}\text{Re}\left[\alpha_{\alpha\alpha}\alpha_{\beta\beta}^*\right], \tag{15}$$

$$\boldsymbol{\alpha G} = \frac{1}{9}\text{Im}\left[\alpha_{\alpha\alpha}G_{\beta\beta}^*\right], \tag{16}$$

$$\beta(\boldsymbol{\alpha})^2 = \frac{1}{2}\text{Re}\left[3\alpha_{\alpha\beta}\alpha_{\alpha\beta}^* - \alpha_{\alpha\alpha}\alpha_{\beta\beta}^*\right], \tag{17}$$

$$\beta(\boldsymbol{G})^2 = \frac{1}{2}\mathrm{Im}\left[3\alpha_{\alpha\beta}G^*_{\alpha\beta} - \alpha_{\alpha\alpha}G^*_{\beta\beta}\right], \tag{18}$$

$$\beta(\boldsymbol{A})^2 = \frac{1}{2}\omega\mathrm{Im}\left[i\alpha_{\alpha\beta}\left(\epsilon_{\alpha\gamma\delta}A_{\gamma,\delta\beta}\right)^*\right]. \tag{19}$$

For a Raman backscattering geometry, S_p is given by[85]

$$S_p = \frac{45\boldsymbol{\alpha}_p^2 + 7\beta(\boldsymbol{\alpha})_p^2}{45}, \tag{20}$$

for a ROA backscattering geometry, it is given by[85]

$$S_p = \frac{48\beta(\boldsymbol{G})_p^2 + \beta(\boldsymbol{A})_p^2/3}{90c}, \tag{21}$$

and for a ROA forward scattering geometry, it is given by[85]

$$S_p = \frac{8(45(\boldsymbol{\alpha G})_p + \beta(\boldsymbol{G})_p^2 - \beta(\boldsymbol{A})_p^2/3)}{90c}. \tag{22}$$

Within the approximations made, the tensor components in Eqs. (15)–(19) are replaced by the first derivative of the purely electronic tensor with respect to the normal mode coordinate p,

$$\alpha_{\alpha\beta} \to \left(\frac{\partial\alpha^{\mathrm{el}}_{\alpha\beta}}{\partial q_p}\right)_{q=q_0}, \tag{23}$$

$$G_{\alpha\beta} \to \left(\frac{\partial G^{\mathrm{el}}_{\alpha\beta}}{\partial q_p}\right)_{q=q_0}, \tag{24}$$

$$A_{\alpha,\beta\gamma} \to \left(\frac{\partial A^{\mathrm{el}}_{\alpha,\beta\gamma}}{\partial q_p}\right)_{q=q_0}, \tag{25}$$

where the "electronic" tensors are those given in Eqs. (10)–(12).

B. Propagator formalism and real time propagation expressions

In order to treat LR-TDDFT and RT-TDDFT on equal footing, it is advantageous to introduce a propagator formalism for the linear response functions:[95] The propagator $\langle\langle\hat{B};\hat{A}\rangle\rangle_\omega$ of an observable $\hat{B}$ with respect to e.g., a time dependent electric field perturbation in the dipole approximation according to $\hat{H}_1(t) = -\hat{A}E(t)$ is implicitly defined in the time domain as[96]

$$\langle\hat{B}(t)\rangle - \langle\hat{B}\rangle_0 = \int_{-\infty}^{t} \mathrm{d}t' \, \langle\langle\hat{B}(t);\hat{A}(t')\rangle\rangle E(t'), \tag{26}$$

where $\langle\hat{B}(t)\rangle = \mathrm{Tr}\left[\rho(t)\hat{B}\right]$ is the time dependent expectation value and $\langle\hat{B}\rangle_0 = \mathrm{Tr}\left[\rho_0\hat{B}\right]$ is the expectation value of the stationary unperturbed system, with the time dependent density $\rho(t)$ and the stationary density ρ_0, respectively. The time domain representation of the propagator, $\langle\langle\hat{B}(t);\hat{A}(t')\rangle\rangle$, is related to its energy domain representation $\langle\langle\hat{B};\hat{A}\rangle\rangle_\omega$ via a Fourier transform (FT). Note that if there is just one perturbation applied, the time domain propagator only depends on differences $t - t'$,[96] which is not apparent from our notation $[\hat{A}(t')$ is to be read as follows: $\hat{A}$ applied carrying the time dependence given by $E(t)$ at time $t']$. The energy domain propagator can then be obtained from a real time propagation scheme via FTs as[96]

$$\langle\langle\hat{B};\hat{A}\rangle\rangle_\omega = \langle\hat{B}(\hbar\omega)\rangle/E(\hbar\omega), \tag{27}$$

where[96]

$$\langle\hat{B}(\hbar\omega)\rangle = \lim_{\epsilon\to 0^+}\int_{-\infty}^{\infty}\mathrm{d}t\left(\langle\hat{B}(t)\rangle - \langle\hat{B}\rangle_0\right)e^{i(\hbar\omega)/\hbar\, t}e^{-\epsilon\, t}. \tag{28}$$

ϵ is a damping factor that can be identified with Γ in Eqs. (10)–(12). In linear response, using the Kubo formula,[97] one can also derive the first order perturbation theory expression as[95,96]

$$\langle\langle\hat{B};\hat{A}\rangle\rangle_\omega = \lim_{\epsilon\to 0^+}\sum_k \frac{1}{\hbar}\left[\frac{\langle 0|\hat{B}|k\rangle\langle k|\hat{A}|0\rangle}{\omega - (\omega_k - \omega_0) + i\epsilon} + \frac{\langle 0|\hat{A}|k\rangle\langle k|\hat{B}|0\rangle}{-\omega - (\omega_k - \omega_0) + i\epsilon}\right]. \tag{29}$$

The relation to Sec. II A is easily seen by replacing the operators $\hat{A}$ and $\hat{B}$ appropriately: The optical linear response tensors are related to the propagators as

$$\alpha^{\mathrm{el}}_{\alpha\beta} = -\langle\langle\hat{d}_\alpha;\hat{d}_\beta\rangle\rangle_\omega, \tag{30}$$

$$G^{\mathrm{el}}_{\alpha\beta} = -\langle\langle\hat{d}_\alpha;\hat{m}_\beta\rangle\rangle_\omega, \tag{31}$$

$$A^{\mathrm{el}}_{\alpha,\beta\gamma} = -\langle\langle\hat{d}_\alpha;\hat{\theta}_{\beta\gamma}\rangle\rangle_\omega. \tag{32}$$

In a practical RT-TDDFT calculation, it is convenient to obtain the optical linear response tensors by perturbing the system according to the electric dipole operator $\hat{A} = \hat{d}_\alpha$ and observing the electric dipole, the magnetic dipole, and the electric quadrupole response during the propagation giving the propagators $\langle\langle\hat{m}_\beta;\hat{d}_\alpha\rangle\rangle_\omega$ and $\langle\langle\hat{\theta}_{\beta\gamma};\hat{d}_\alpha\rangle\rangle_\omega$ for the magnetic dipole response and the electric quadrupole response, respectively. In terms of Eqs. (1)–(3), this corresponds to a calculation of $\mathscr{G}^{\mathrm{el}}_{\alpha\beta}$ and $\mathscr{A}^{\mathrm{el}}_{\alpha,\beta\gamma}$ instead of $G^{\mathrm{el}}_{\alpha\beta}$ and $A^{\mathrm{el}}_{\alpha,\beta\gamma}$, respectively. However, the short time approximation, effectively setting $\omega_S = \omega_I$ in Eq. (4), allows simple relations between these tensors:[86] The tensors are related as $i\mathscr{G}^{\mathrm{el}}_{\alpha\beta} = -G^{\mathrm{el}}_{\alpha\beta}$ and $\mathscr{A}^{\mathrm{el}}_{\alpha,\beta\gamma} = A^{\mathrm{el}}_{\alpha,\beta\gamma}$ (in the absence of a static magnetic field).[85]

The derivatives necessary for Eqs. (23)–(25) can be performed numerically according to the scheme used in Refs. 65 and 93.

C. Representations, magnetic response, and nonlocal potentials

The equation of motion for the propagators,[95,96]

$$\begin{aligned}\hbar\omega\langle\langle\hat{B};\hat{A}\rangle\rangle_\omega &= \langle[\hat{B},\hat{A}]\rangle_0 + \langle\langle[\hat{B},H];\hat{A}\rangle\rangle_\omega \\ &= \langle[\hat{B},\hat{A}]\rangle_0 + \langle\langle B;[H,\hat{A}]\rangle\rangle_\omega,\end{aligned} \tag{33}$$

allows us to switch between the length, mixed, and velocity representations of the linear response tensors (see Appendix A). Note that these equations are exactly fulfilled only for a complete basis set as they involve a commutator.[98] In linear response, the different representations of the polarizabilities correspond to different (equivalent) choices of gauge in the electric dipole approxima-

tion;[99,100] it is only when approximations are made that different representations (or choices of gauge) lead to different results.[101–103]

In order to retain the gauge invariance of the time dependent Kohn–Sham equations in the presence of nonlocal potentials[79–81,104] it is necessary to use a modified version of the momentum operator,

$$\hat{p}_\alpha^{\text{gen}} = \frac{m_e}{i\hbar}[\hat{r}_\alpha, \hat{H}] = \hat{p}_\alpha + \frac{m_e}{i\hbar}[\hat{r}_\alpha, \hat{V}^{\text{nl}}], \tag{34}$$

as discussed for RT-TDDFT in Ref. 82. This also affects the definition of the magnetic dipole moment operator in Eq. (6), where this modified definition holds to first order in a magnetic field perturbation.[79–81,83] A table of different representations of the linear response functions $\boldsymbol{\alpha}$, $\mathscr{G}$, and $\mathscr{A}$ can be found in Table I in the Appendix.

D. Origin dependence

In a finite basis set, the calculation of ROA spectra in principle shows an origin dependence. In order to alleviate that, we use the velocity representations of the electric dipole moment operator[28,56,60] (and the electric quadrupole moment operator). The response tensors $\boldsymbol{G}$ and $\boldsymbol{A}$ are naturally origin dependent, since the magnetic dipole moment operator in Eq. (6) and the electric quadrupole operator in Eq. (7) are origin dependent for a shift of the origin from $\vec{O}$ to $\vec{O} + \vec{a}$ (the electric dipole moment is origin independent for neutral systems),

$$\hat{m}_\alpha^{\text{gen},O+a} = \hat{m}_\alpha^{\text{gen},O} + \frac{e}{2m_e}\epsilon_{\alpha\beta\gamma}a_\beta\hat{p}_\gamma^{\text{gen}}, \tag{35}$$

$$\hat{Q}_{\alpha\beta}^{O+a} = -e\left(\hat{r}_\alpha^{O+a}\hat{r}_\beta^{O+a}\right) = -e\left(\hat{r}_\alpha^O\hat{r}_\beta^O - a_\beta\hat{r}_\alpha^O - a_\alpha\hat{r}_\beta^O + a_\alpha a_\beta\right), \tag{36}$$

$$\hat{Q}_{\alpha\beta}^{\text{vel},O+a} = \hat{Q}_{\alpha\beta}^{\text{vel},O} - ea_\alpha\hat{p}_\beta^{\text{gen}} - ea_\beta\hat{p}_\alpha^{\text{gen}}, \tag{37}$$

where we switched to the *second moment* definition of the electric quadrupole moment in its length and velocity representation,[98,105,106]

$$\hat{Q}_{\alpha\beta}^{O} = -e\left(\hat{r}_\alpha^O\hat{r}_\beta^O\right), \tag{38}$$

$$\hat{Q}_{\alpha\beta}^{\text{vel},O} = -e\left(\hat{r}_\alpha^O\hat{p}_\beta^{\text{gen}} + \hat{p}_\alpha^{\text{gen}}\hat{r}_\beta^O\right). \tag{39}$$

Linear response functions needed for $\boldsymbol{G}$ show the following origin dependence in the length and velocity representations:

$$\langle\langle\hat{r}_\alpha^{O+a}; \hat{m}_\beta^{\text{gen},O+a}\rangle\rangle_\omega = \langle\langle\hat{r}_\alpha^{O}; \hat{m}_\beta^{\text{gen},O}\rangle\rangle_\omega + \frac{e}{2m_e}\epsilon_{\beta\gamma\delta}a_\gamma\langle\langle\hat{r}_\alpha^{O}; \hat{p}_\delta^{\text{gen}}\rangle\rangle_\omega, \tag{40}$$

$$\langle\langle\hat{p}_\alpha^{\text{gen},O+a}; \hat{m}_\beta^{\text{gen},O+a}\rangle\rangle_\omega = \langle\langle\hat{p}_\alpha^{\text{gen}}; \hat{m}_\beta^{\text{gen},O}\rangle\rangle_\omega + \frac{e}{2m_e}\epsilon_{\beta\gamma\delta}a_\gamma\langle\langle\hat{p}_\alpha^{\text{gen}}; \hat{p}_\delta^{\text{gen}}\rangle\rangle_\omega, \tag{41}$$

as well as the following for $\boldsymbol{A}$ in its different representations:

$$\begin{aligned}\langle\langle\hat{r}_\alpha^{O+a}; \hat{Q}_{\beta\gamma}^{O+a}\rangle\rangle_\omega = \langle\langle\hat{r}_\alpha^{O}; \hat{Q}_{\beta\gamma}^{O}\rangle\rangle_\omega - ea_\beta\langle\langle\hat{r}_\alpha^{O}; \hat{r}_\gamma^{O}\rangle\rangle_\omega \\ - ea_\gamma\langle\langle\hat{r}_\alpha^{O}; \hat{r}_\beta^{O}\rangle\rangle_\omega,\end{aligned} \tag{42}$$

$$\begin{aligned}\langle\langle\hat{p}_\alpha^{\text{gen},O+a}; \hat{Q}_{\beta\gamma}^{O+a}\rangle\rangle_\omega = \langle\langle\hat{p}_\alpha^{\text{gen}}; \hat{Q}_{\beta\gamma}^{O}\rangle\rangle_\omega - ea_\beta\langle\langle\hat{p}_\alpha^{\text{gen}}; \hat{r}_\gamma^{O}\rangle\rangle_\omega \\ - ea_\gamma\langle\langle\hat{p}_\alpha^{\text{gen}}; \hat{r}_\beta^{O}\rangle\rangle_\omega,\end{aligned} \tag{43}$$

$$\begin{aligned}\langle\langle\hat{r}_\alpha^{O+a}; \hat{Q}_{\beta\gamma}^{\text{vel},O+a}\rangle\rangle_\omega = \langle\langle\hat{r}_\alpha^{O}; \hat{Q}_{\beta\gamma}^{\text{vel},O}\rangle\rangle_\omega - ea_\beta\langle\langle\hat{r}_\alpha^{O}; \hat{p}_\gamma^{\text{gen}}\rangle\rangle_\omega \\ - ea_\gamma\langle\langle\hat{r}_\alpha^{O}; \hat{p}_\beta^{\text{gen}}\rangle\rangle_\omega,\end{aligned} \tag{44}$$

$$\begin{aligned}\langle\langle\hat{p}_\alpha^{\text{gen},O+a}; \hat{Q}_{\beta\gamma}^{\text{vel},O+a}\rangle\rangle_\omega = \langle\langle\hat{p}_\alpha^{\text{gen}}; \hat{Q}_{\beta\gamma}^{\text{vel},O}\rangle\rangle_\omega - ea_\beta\langle\langle\hat{p}_\alpha^{\text{gen}}; \hat{p}_\gamma^{\text{gen}}\rangle\rangle_\omega \\ - ea_\gamma\langle\langle\hat{p}_\alpha^{\text{gen}}; \hat{p}_\beta^{\text{gen}}\rangle\rangle_\omega.\end{aligned} \tag{45}$$

Note that $\hat{p}_\alpha^{\text{gen}}$ shows no origin dependence,

$$\begin{aligned}\hat{p}_\alpha^{\text{gen},O+a} &= \hat{p}_\alpha^{O} + \frac{m_e}{i\hbar}[\hat{r}_\alpha - a_\alpha, \hat{V}^{\text{nl}}] \\ &= \hat{p}_\alpha + \frac{m_e}{i\hbar}[\hat{r}_\alpha, \hat{V}^{\text{nl}}] - \frac{m_e}{i\hbar}[a_\alpha, \hat{V}^{\text{nl}}],\end{aligned} \tag{46}$$

where the last term is canceled since a_α is just a constant, and the momentum operator is origin independent.

With the different representations in Eqs. (40)–(45) at hand, the origin dependence of the invariants in Eqs. (15)–(19) can be examined in the STA described in Sec. II A. We assume that the derivatives of the response tensors in Eqs. (23)–(25) show the same symmetries and transformation properties as the electronic response tensors themselves, which is reasonable in our finite difference scheme.

TABLE I. Different representations of the propagators for a practical RT-TDDFT calculation of the linear response tensors including non-local potentials.

Propagator	Perturbation	Measurement	Response tensor
$\langle\langle\hat{r}_\alpha;\hat{r}_\beta\rangle\rangle_\omega$	$\hat{r}_\beta$	$\hat{r}_\alpha$	$\alpha_{\alpha\beta}$
$\langle\langle\hat{r}_\alpha;\hat{p}_\beta^{\text{gen}}\rangle\rangle_\omega$	$\hat{p}_\beta^{\text{gen}}$	$\hat{r}_\alpha$	$\alpha_{\alpha\beta}$
$\langle\langle\hat{p}_\alpha^{\text{gen}};\hat{r}_\beta\rangle\rangle_\omega$	$\hat{r}_\beta$	$\hat{p}_\alpha^{\text{gen}}$	$\alpha_{\alpha\beta}$
$\langle\langle\hat{p}_\alpha^{\text{gen}};\hat{p}_\beta^{\text{gen}}\rangle\rangle_\omega$	$\hat{p}_\beta^{\text{gen}}$	$\hat{p}_\alpha^{\text{gen}}$	$\alpha_{\alpha\beta}$
$\langle\langle\hat{m}_\alpha^{\text{gen}};\hat{r}_\beta\rangle\rangle_\omega$	$\hat{r}_\beta$	$\hat{m}_\alpha^{\text{gen}}$	$\mathscr{G}_{\alpha\beta}$
$\langle\langle\hat{m}_\alpha^{\text{gen}};\hat{p}_\beta^{\text{gen}}\rangle\rangle_\omega$	$\hat{p}_\beta^{\text{gen}}$	$\hat{m}_\alpha^{\text{gen}}$	$\mathscr{G}_{\alpha\beta}$
$\langle\langle\hat{r}_\alpha\hat{r}_\beta;\hat{r}_\gamma\rangle\rangle_\omega$	$\hat{r}_\gamma$	$\hat{r}_\alpha\hat{r}_\beta$	$\mathscr{A}_{\gamma,\alpha\beta}$
$\langle\langle\hat{r}_\alpha\hat{r}_\beta;\hat{p}_\gamma^{\text{gen}}\rangle\rangle_\omega$	$\hat{p}_\gamma^{\text{gen}}$	$\hat{r}_\alpha\hat{r}_\beta$	$\mathscr{A}_{\gamma,\alpha\beta}$
$\langle\langle\hat{r}_\alpha\hat{p}_\beta^{\text{gen}} + \hat{p}_\alpha^{\text{gen}}\hat{r}_\beta;\hat{r}_\gamma\rangle\rangle_\omega$	$\hat{r}_\gamma$	$\hat{r}_\alpha\hat{p}_\beta^{\text{gen}} + \hat{p}_\alpha^{\text{gen}}\hat{r}_\beta$	$\mathscr{A}_{\gamma,\alpha\beta}$
$\langle\langle\hat{r}_\alpha\hat{p}_\beta^{\text{gen}} + \hat{p}_\alpha^{\text{gen}}\hat{r}_\beta;\hat{p}_\gamma^{\text{gen}}\rangle\rangle_\omega$	$\hat{p}_\gamma^{\text{gen}}$	$\hat{r}_\alpha\hat{p}_\beta^{\text{gen}} + \hat{p}_\alpha^{\text{gen}}\hat{r}_\beta$	$\mathscr{A}_{\gamma,\alpha\beta}$

Since the invariants contain products of tensor components, the different representations give rise to many combinations: $\boldsymbol{\alpha}$ can be represented in a length, two mixed, and a velocity representation, $\boldsymbol{G}$ in a length and a mixed representation, and $\boldsymbol{A}$ again in a length, two mixed, and a velocity representation (see Table I), which means that, e.g., there are 16 possible representations for $\beta(\boldsymbol{A})^2$, for a perturbation according to the dipole approximation. Some examples are spelled out in Appendix B. Analyzing these expressions leads to the following conditions for the representations of $\alpha_{\alpha\beta}$, in order for the invariants to be origin independent: First,

$$\langle\langle \hat{A}_\alpha; \hat{B}_\beta \rangle\rangle_\omega^* \stackrel{!}{=} \langle\langle \hat{A}_\beta; \hat{B}_\alpha \rangle\rangle_\omega^*, \tag{47}$$

which states basically the symmetry of $\alpha_{\alpha\beta}$. Second, for $\beta(\boldsymbol{G})^2$ and $\beta(\boldsymbol{A})^2$, the condition

$$\langle\langle \hat{A}_\alpha; \hat{B}_\beta \rangle\rangle_\omega \langle\langle \hat{C}_\gamma; \hat{D}_\delta \rangle\rangle_\omega^* \stackrel{!}{=} \langle\langle \hat{A}_\gamma; \hat{B}_\delta \rangle\rangle_\omega \langle\langle \hat{C}_\alpha; \hat{D}_\beta \rangle\rangle_\omega^* \tag{48}$$

needs to be matched, which is a kind of "supersymmetry" in a product of two linear response functions.

The operators $\hat{A}$, $\hat{B}$, $\hat{C}$, and $\hat{D}$ are placed holders for either $\hat{r}$ or $\hat{p}^{\text{gen}}$. For a finite basis set, the first condition is only exactly fulfilled if $\hat{A} = \hat{B}$. Consequently, for $\boldsymbol{\alpha G}$, the velocity representation of $G_{\alpha\beta}$ has to be used [see Eqs. (B1) and (B3)].

To investigate the condition in Eq. (48), one can show that, for the complex conjugate of the linear response functions, the following relation holds:[96,98,107]

$$\langle\langle \hat{A}; \hat{B} \rangle\rangle_\omega^* = \langle\langle \hat{A}; \hat{B} \rangle\rangle_{-\omega}^* = \langle\langle \hat{B}; \hat{A} \rangle\rangle_\omega. \tag{49}$$

This equation holds irrespective of the basis set size, since it does not involve a commutator and is basically a consequence of the hermiticity of the observables. Thus, the condition in Eq. (48) can be rewritten as

$$\langle\langle \hat{D}_\delta; \hat{C}_\gamma \rangle\rangle_\omega \langle\langle \hat{B}_\beta; \hat{A}_\alpha \rangle\rangle_\omega^* \stackrel{!}{=} \langle\langle \hat{A}_\gamma; \hat{B}_\delta \rangle\rangle_\omega \langle\langle \hat{C}_\alpha; \hat{D}_\beta \rangle\rangle_\omega^*. \tag{50}$$

This condition is fulfilled if

1. $\hat{A} = \hat{D}$, $\hat{C} = \hat{B}$, and
2. generally $\langle\langle \hat{A}_\alpha; \hat{B}_\beta \rangle\rangle_\omega = \langle\langle \hat{A}_\beta; \hat{B}_\alpha \rangle\rangle_\omega$, which is again the condition in Eq. (47), implying $\hat{A} = \hat{B}$ and $\hat{C} = \hat{D}$.

For an origin independent calculation of $\beta(\boldsymbol{G})^2$ in a finite basis set, this implies that both $\boldsymbol{\alpha}$ and $\boldsymbol{G}$ have to be calculated in the velocity representation [see Eq. (B7)]. For an origin independent calculation of $\beta(\boldsymbol{A})^2$ in a finite basis set, there are two possibilities since the origin dependent term in the length representation [see Eq. (42)] only involves position operators. Thus, for $\beta(\boldsymbol{A})^2$, both $\boldsymbol{\alpha}$ and $\boldsymbol{A}$ have to be calculated either in their length or in their velocity representations consistently.

In conclusion, one can see that

- for $\boldsymbol{\alpha G}$ the velocity representation of $\boldsymbol{G}$,
- for $\beta(\boldsymbol{G})^2$ consistently the velocity representation of $\boldsymbol{\alpha}$ and $\boldsymbol{G}$,
- and for $\beta(\boldsymbol{A})^2$ either the length or the velocity representations have to be used for both $\boldsymbol{\alpha}$ and $\boldsymbol{A}$ consistently

in order to achieve the origin independence in a finite basis set, analogous to previous works using LR-TDDFT.[28,56,60] Note that in the presence of nonlocal potentials, the use of the generalized momentum [Eq. (34)] is implied.

III. COMPUTATIONAL DETAILS

The RT-TDDFT calculations were carried out with the package CP2K.[68–70,108] Continuing our previous efforts for the implementation of $\boldsymbol{G}$ in various representations,[82] the velocity representation of $\boldsymbol{A}$ was also implemented into CP2K. For the numerical integration of the time dependent Kohn–Sham equations, the Hamiltonian is extrapolated in time by the always-stable predictor corrector algorithm and several options are available for the approximation of the propagator and the calculation of the matrix exponential. If not mentioned otherwise, we chose the enforced time reversible symmetry scheme for the propagation and an Arnoldi subspace algorithm for the calculation of the matrix exponential. As a time step for the propagation, we chose 0.1 a.u. in order to cover a sufficiently large frequency range after the Fourier transform to describe all excitations the Fourier transform. As the damping factor ϵ in Eq. (28) we chose 0.1 eV ≈ 0.0036 a.u. in order to match the experimental line width in the absorption spectrum. The calculations were run at least for a total simulation time of 3000 a.u. An investigation off the dependence of the spectrum on the amount of simulation time was given in Ref. 65.

The external field is applied in the form of a δ-pulse in the dipole approximation, in order to excite all transitions in the system. In the length gauge,[103] corresponding to the length representation, this is done by applying $\kappa_\alpha = I_\alpha/\hbar$ to the ground state molecular orbitals (in atomic units),[109]

$$|\phi(t = 0_+)\rangle = e^{i\kappa_\alpha \hat{r}_\alpha} |\phi(t = 0_-)\rangle, \tag{51}$$

where I_α is an impulse in the α direction. In the velocity gauge, corresponding to the velocity representation, the interaction term to the first order is proportional to $\hat{p}_\alpha$.[103] The pulse is then applied by using first order density functional perturbation theory (*Sternheimer's equation*) on the ground state molecular orbitals, in terms of orbitals (in atomic units),

$$\left|\phi_i^{\text{pert}}\right\rangle = \sum_{k,\text{virt}} \frac{\langle \phi_k | \kappa_\alpha \hat{p}_\alpha^{\text{gen}} | \phi_i \rangle}{\epsilon_i - \epsilon_k} |\phi_k\rangle, \tag{52}$$

where ϕ_i and ϕ_k represent the ground state occupied and the virtual molecular orbitals and ϵ_i and ϵ_k are their energies, respectively. ϕ_i^{pert} are the starting orbitals for the real time propagation. Note that we here use the *generalized momentum* due to the presence of nonlocal pseudopotentials. During the propagation, all of the observables in Table I were traced and postprocessed in order to obtain the various spectra. Note that in this way, a variety of response tensors and representations can be obtained at once, also for different reference points of the "measured" observables. In our calculations, we do not see the additional expectation values connecting the representations in Eqs. (A3), (A6), and (A5), most likely due to the application of the δ-pulse in a DFPT frame work, which already accounts for a factor of ω. For the calculation of the invariants in different representations, this has also the consequence that we only have to factor in ω as many times as we use a velocity representation for any of the "measurement" observables.

Vibrational spectra in the STA were calculated according to the numerical scheme as in previous works.[65,93]

In all calculations, we used the PBE exchange–correlation functional[110] and either the aug-QZV2P-GTH basis set[111] or the TZVP-GTH basis set[111] in combination with GTH pseudopotentials.[112]

The vibrational spectra are broadened by Lorentzians with a full width at half maximum height of 20 cm^{-1}. The vibrational spectra were calculated according to Eq. (13) at a temperature of 300 K.

IV. RESULTS

This section is structured as follows: First, the absorption and ECD spectra of the (R)-methyloxirane molecule are given. Second, the origin dependence of the ROA invariants is evaluated, and afterward, the Raman and ROA spectra are presented and discussed.

A. Absorption and ECD spectrum

The RT-TDDFT absorption and ECD spectra of (R)-methyloxirane are shown in Fig. 1. The first and second excitations are found at 5.69 eV and 6.14 eV, respectively. Note that these values are exchange-correlation functional and basis set dependent. Experimental absorption and ECD spectra of (R)-methyloxirane can be found in Refs. 65 and 93 and agree qualitatively with our RT-TDDFT results, with the first excitation found at higher energies than in our calculations. However, in order to consistently treat resonance spectra, we choose the excitation at 5.69 eV (218 nm) for the calculation of the vibrational spectra in Sec. IV C.

B. Origin dependence of the invariants

In order to investigate the origin dependence of the invariants within the STA, the derivatives of the (RT-TDDFT) response tensors [compare Eqs. (23)–(25)] were calculated with the origin of the coordinate system set either to the center of mass (c.o.m.) of the molecule or to the origin of the simulation cell, which corresponds to a shift of 12.83 Å. The results are shown below for different representations of the invariants containing derivatives of the origin dependent $\boldsymbol{G}$ and $\boldsymbol{A}$. For the comparison of the different representations, we use the TZVP-GTH basis set when the generalized momentum is included and the aug-QZV2P-GTH basis set if it is not included. In this way, we minimize the effects of the finite basis set, which allows for a clearer analysis of the influence of the generalized momentum. Because of the basis set dependence of the ROA invariants, the invariants calculated for different basis sets are not directly comparable.

As a short notation for the representations of the invariants, we introduce an intuitive four letter code, where the first two letters always encode the representation of $\boldsymbol{\alpha}$ and the last two letters the remaining linear response tensor, e.g., for $\boldsymbol{\alpha G}$, "ppmr" means $\boldsymbol{\alpha}$ in the velocity representation and $\boldsymbol{G}$ in the length representation and for $\beta(\boldsymbol{A})^2$, "prqp" means a mixed representation for $\boldsymbol{\alpha}$ (pulse: length rep., measurement: velocity rep.) and also a mixed representation of $\boldsymbol{A}$ (pulse: velocity rep., measurement: length rep.). We will also use the term "representations" for this four-letter short hand notion. The short hand notation for the quadrupole moment is "q," and for its velocity representation, it is "v." For pseudopotentials, the extra commutator is always included implicitly, if not mentioned otherwise.

Note that the RT-TDDFT approach allows us to evaluate the dependence of the invariants on the whole excitation frequency range within just one set of simulations.

The invariants shown in this subsection are calculated for the normal mode of (R)-methyloxirane with a wavenumber of 1146 cm^{-1} (aug-QZV2P-GTH) or 1145 cm^{-1} (TZVP-GTH).

1. Invariants αG and $\beta(G)^2$

Different representations of $\alpha G(\omega)$ are shown in Fig. 2 for the TZVP-GTH basis set. Comparing the invariants for representations involving either a length or a velocity representation of $\boldsymbol{G}$, one observes a slight origin dependence, whenever the length representation of $\boldsymbol{G}$ is used. If $\boldsymbol{G}$ is calculated in the velocity representation, it does not make any difference which representation of $\boldsymbol{\alpha}$ is used, as expected from theory.

In order to investigate the importance of the generalized momentum, the same invariants are calculated for a case, where it was not taken into account for the "measurements" of the observables. The results are shown in Fig. 3. In this case, we see a significant origin dependence of $\boldsymbol{\alpha G}$, although we are already close to the basis set limit with the aug-QZV2P-GTH basis set. This emphasizes the necessity of using the generalized momentum in the presence of nonlocal potential, consistent with our previous results for the simulation of ECD spectra.[82]

In Fig. 4, different representations of $\beta(\boldsymbol{G})^2$ are given. Again an origin dependence is observed, if $\boldsymbol{G}$ is used in the length

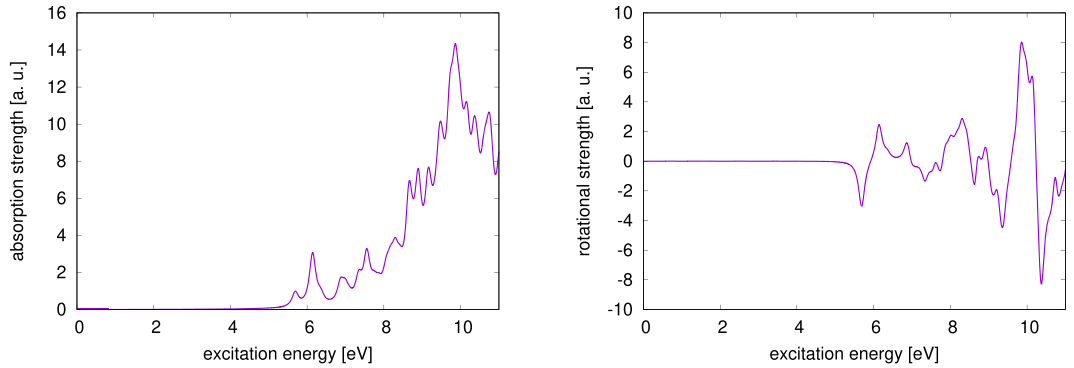

FIG. 1. Absorption (a) and ECD (b) spectra of (R)-methyloxirane for the aug-QZV2P-GTH basis set, already published by the authors in Ref. 82.

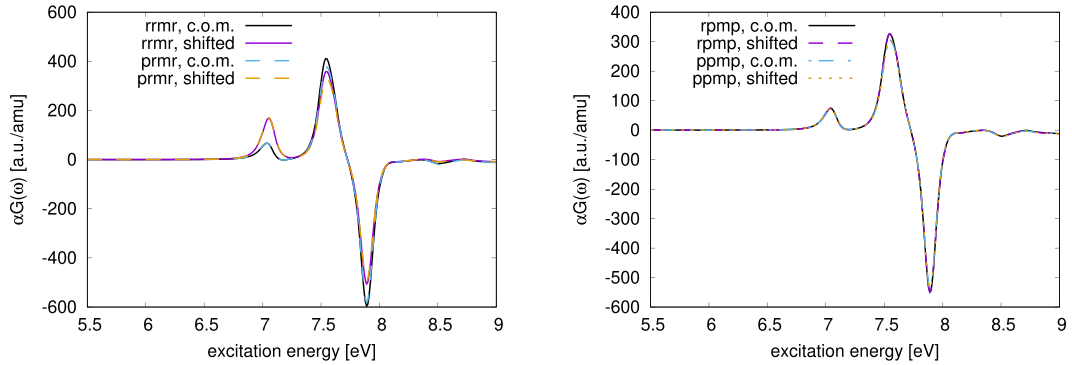

FIG. 2. $\boldsymbol{\alpha G}$ in different representations for different coordinate origins. The generalized momentum is used wherever applicable. The notation for the representations is given in Sec. IV B.

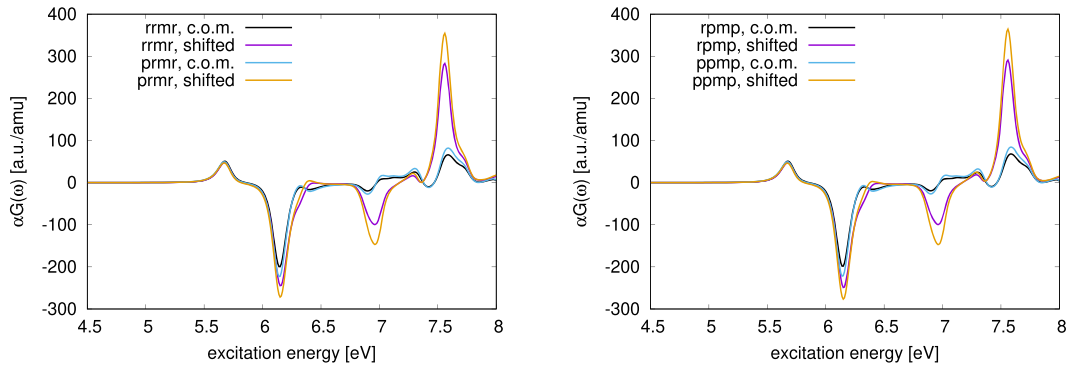

FIG. 3. $\boldsymbol{\alpha G}$ in different representations for different coordinate origins. The generalized momentum is not used.

representation. In contrast to the investigation of $\boldsymbol{\alpha G}$, the representation of $\boldsymbol{\alpha}$ cannot be chosen arbitrarily, as illustrated by the origin dependence of the "rpmp" representation on the right hand side (RHS) of Fig. 4. In fact, only the "ppmp" representation shows no origin dependence, consistent with the theoretical results. Again, we investigate the importance of the generalized momentum by not including it for the measurement of the observables. The resulting invariants are shown in Fig. 5. As for $\boldsymbol{\alpha G}$, omitting the

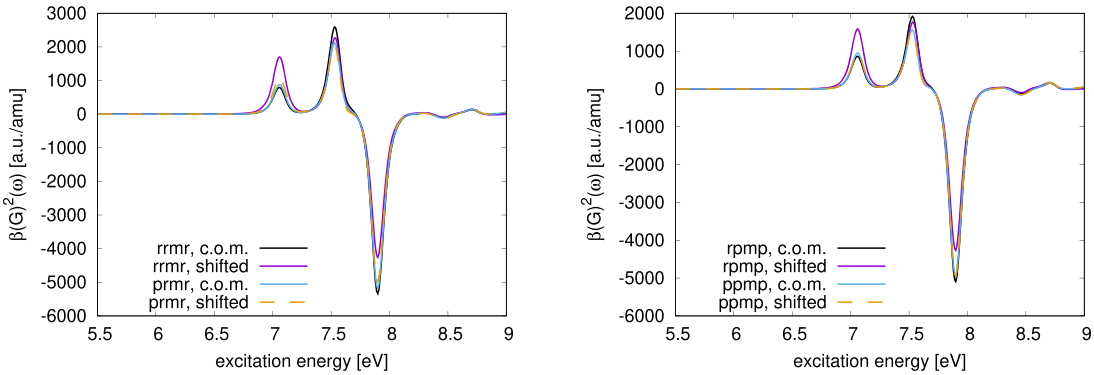

FIG. 4. $\beta(\boldsymbol{G})^2$ in different representations for different coordinate origins. The generalized momentum is used wherever applicable.

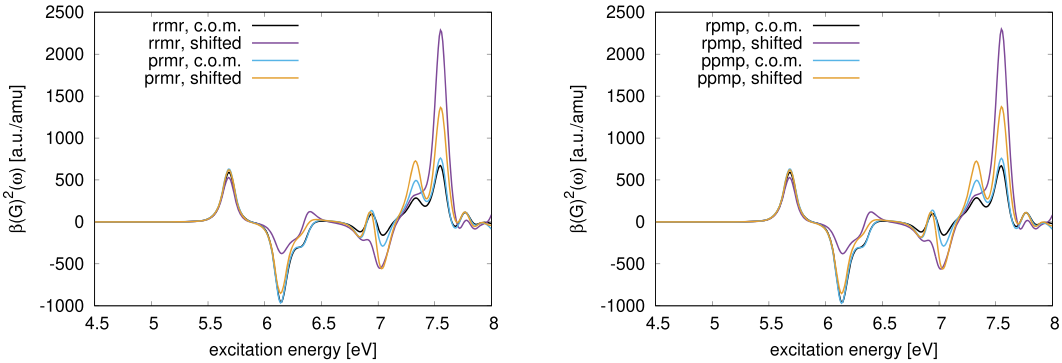

FIG. 5. $\beta(\boldsymbol{G})^2$ in different representations for different coordinate origins. The generalized momentum is not used.

generalized momentum leads to a remarkable origin dependence of $\beta(\boldsymbol{G})^2$ in all its representations, despite the rather large basis set (aug-QZV2P-GTH).

2. $\beta(\boldsymbol{A})^2$

Different representations of $\beta(\boldsymbol{A})^2$ are shown in Fig. 6. As expected, representations of the invariant involving either the length or the velocity representations of $\boldsymbol{\alpha}$ and $\boldsymbol{A}$ consistently do not show any origin dependence, within the numerical accuracy of the method, whereas all other representations of $\beta(\boldsymbol{A})^2$ show a significant origin dependence, consistent with the theoretical results in Sec. II D. Investigating the role of the generalized momentum, the same representations as in Fig. 6 are shown in Fig. 7 for the aug-QZV2P-GTH basis set, without taking the generalized momentum into account for the "measurements" of the observables. In this case, only the "rrqr" representation does not show any origin dependence, because it does not involve the momentum operator. As before, all other representations show a significant origin dependence, if the generalized momentum is omitted.

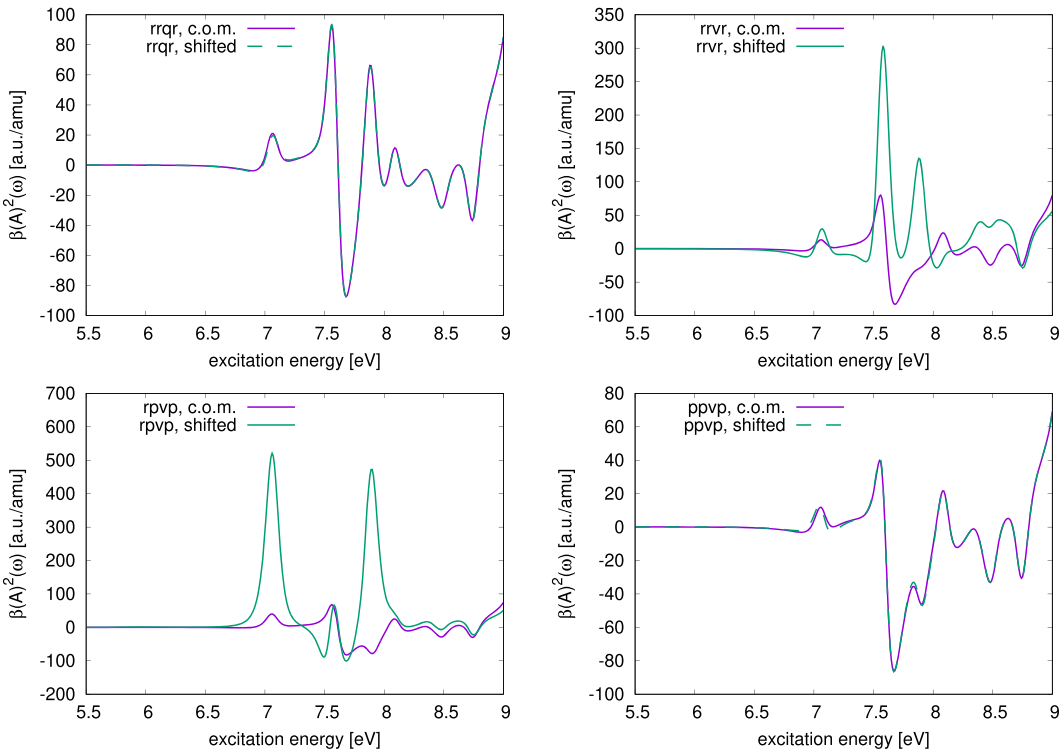

FIG. 6. $\beta(\boldsymbol{A})^2$ in different representations for different coordinate origins. The generalized momentum is used wherever applicable.

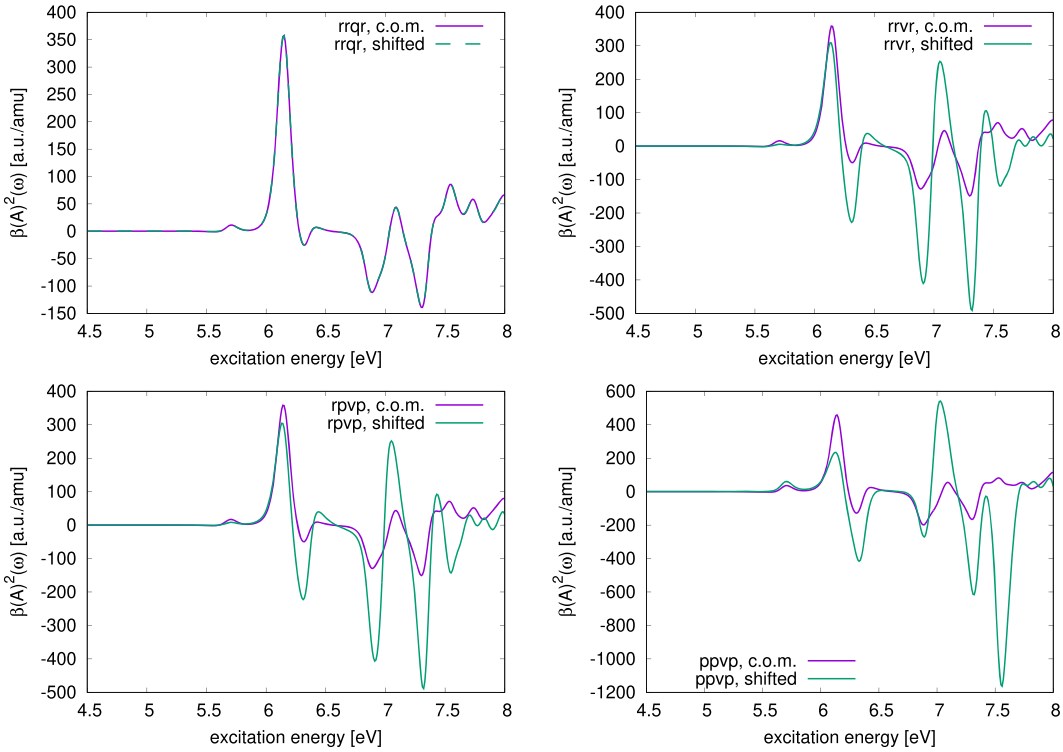

FIG. 7. $\beta(\boldsymbol{A})^2$ in different representations for different coordinate origins. The generalized momentum is not used.

Concerning the calculation of ROA spectra with RTP, it is advantageous to use a velocity representation for the perturbation of the system, since in that case, all invariants can be calculated without origin dependence, and a second run with an electric-dipole perturbation in the length representation can be avoided.

C. Raman and ROA spectra

In this section, nonresonance and resonance Raman and ROA spectra are presented for R-methyloxirane in Figs. 8 and 9, respectively. According to the discussion in Sec. IV B 2, the velocity representation was used for the calculation of $\boldsymbol{\alpha}$, $\boldsymbol{A}$, and $\boldsymbol{G}$. For the nonresonance spectra, the excitation energy was set to 2.41 eV (514 nm), and, for the resonance spectra, the electronic transition at 5.69 eV (218 nm) was chosen as the excitation energy. For both Raman and ROA spectra, a backscattering geometry is assumed; i.e., the spectra are calculated according to Eqs. (20) and (21).

From the Raman spectra in Fig. 8, one can see that the intensity of the resonance spectrum is several orders of magnitude larger

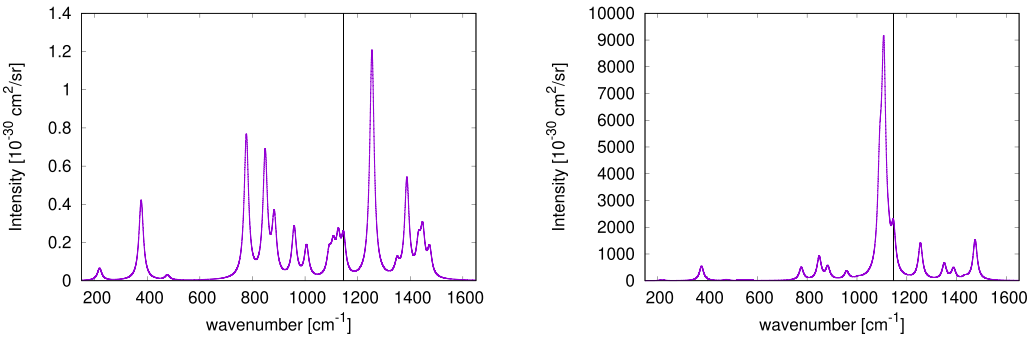

FIG. 8. Nonresonant (left hand side, LHS) and resonant (right hand side, RHS) Raman spectra of R-methyloxirane. The vertical line marks 1146 cm^{-1}.

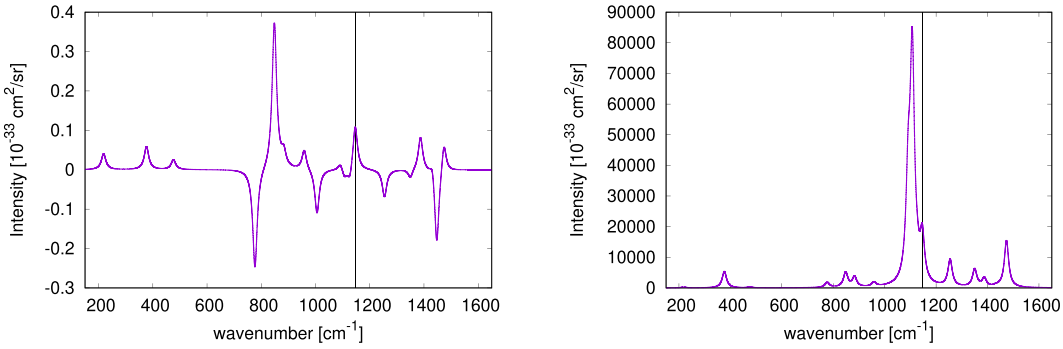

FIG. 9. Nonresonant (LHS) and resonant (RHS) ROA spectra of R-methyloxirane. The vertical line marks 1146 cm^{-1}.

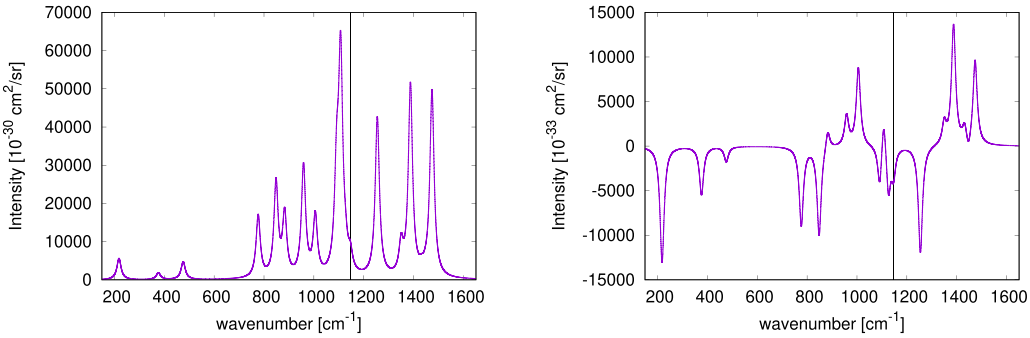

FIG. 10. Resonant Raman (LHS) and resonant (RHS) ROA spectra of R-methyloxirane at an excitation energy of 8.0 eV. The vertical line marks 1146 cm^{-1}.

than that of the nonresonant spectrum, consistent with the experimental observations. The nonresonance spectrum agrees qualitatively well with the gas phase spectrum of (R)-methyloxirane in Ref. 115.

Compared to that, the ROA spectra in Fig. 9 show an intensity several orders of magnitude smaller than that of their Raman counterparts. Nevertheless, the intensity of the resonance ROA spectrum is several orders of magnitude larger than the one of the nonresonance ROA spectrum. Also, its relative intensities are (almost) identical to the corresponding Raman spectrum, which is consistent with the results of a two state approximation to ROA spectroscopy, which states that at resonance with a single excited electronic state, the ROA spectrum shows the same relative intensities as the corresponding Raman spectrum, with a sign opposite to the sign of the rotatory strength at that excitation.[116]

In Fig. 10, the resonant Raman and ROA spectra are shown for an excitation energy of 8.0 eV. As different electronic transitions overlap at this excitation energy, the two state picture, where the ROA spectrum is monosignate at the electronic transition, breaks down and the ROA spectrum shows peaks having different signs. In order to show the different contributions of $\beta(\boldsymbol{G})^2$ and $\beta(\boldsymbol{A})^2$ to this resonant ROA spectrum, the two invariants are shown exemplarily for the normal mode with a wavenumber of 1146 cm^{-1} in Fig. 11. In general, the values of both invariants show the same order of magnitude. However, if one considers the factors in Eq. (21), it becomes apparent that $\beta(\boldsymbol{G})^2$ mainly determines the signs of the peaks. Note that, with a real time propagation approach such as RT-TDDFT, the variation of the values of the invariants can be traced naturally over the whole excitation energy range.

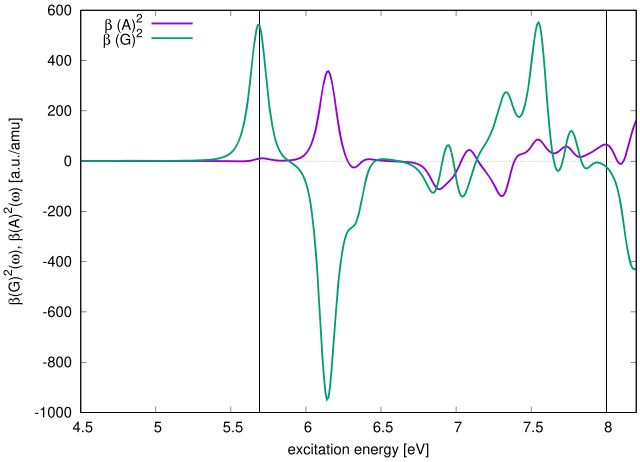

FIG. 11. $\beta(\boldsymbol{G})^2$ and $\beta(\boldsymbol{A})^2$ for the normal mode with a wavenumber of 1146 cm^{-1}. The vertical lines are at 5.69 eV and 8.0 eV.

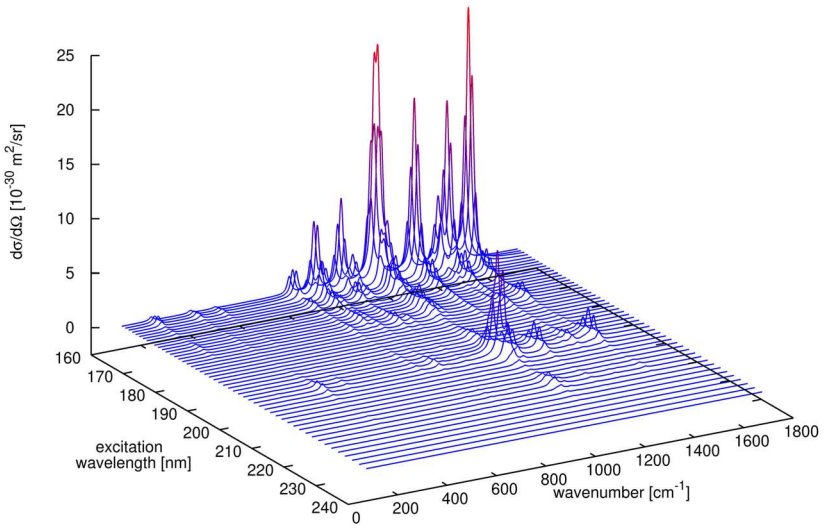

FIG. 12. Raman excitation profile of (R)-methyloxirane (PBE, aug-QZV2P-GTH).

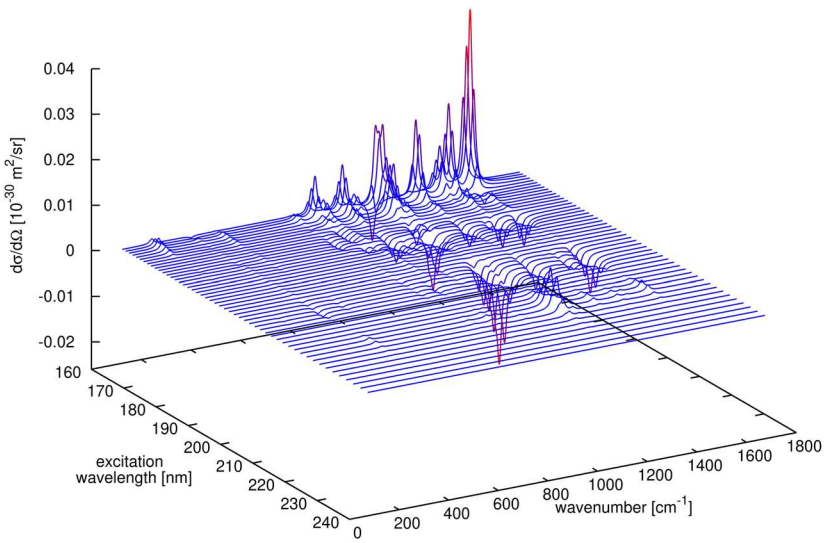

FIG. 13. ROA excitation profile of (R)-methyloxirane (PBE, aug-QZV2P-GTH).

In order to further illustrate the advantage of a time domain approach, we also show the full Raman and ROA excitation profiles in Figs. 12 and 13.

In contrast to LR-TDDFT approaches, these can be obtained with an arbitrary resolution over the whole excitation frequency range from just a single set of simulations.

V. CONCLUSION

The first calculations of ROA spectra with real time propagation have been described, for which the RT-TDDFT method in the CP2K program has been extended. This approach includes off-, pre-, and on resonance effects considering one or more electronically excited state(s), which is highly desirable for the in-depth study of involved systems such as transition metal complexes. A theoretical analysis has been presented with an emphasis on the propagator formulation of the linear response, which allows for a systematic evaluation of the origin dependence of optical linear response tensors. We have found that the ROA invariants involving magnetic linear response functions show no origin dependence within the numerical accuracy of RT-TDDFT for the calculation of vibrational spectra within the short time approximation, if the velocity representation (for the $\boldsymbol{\alpha G}$ invariant, also the mixed and length representations) of the electric-dipole–electric-dipole polarizability and the velocity representation of the electric-dipole–magnetic-dipole polarizability are used. For the invariant involving the electric-dipole–electric-quadrupole polarizability, we have found that both the electric-dipole–electric-dipole polarizability and the electric-dipole–electric-quadrupole polarizability have to be calculated in either the length representation or the

velocity representation in order to achieve an origin independent result, consistent with previous LR-TDDFT results.[28,56,60] These findings establish further the equivalence of LR- and RT-TDDFT in the weak perturbation regime.[65,117] Moreover, the importance of the inclusion of an extra term in the definition of the momentum operator in the presence of nonlocal potentials is emphasized, which is vital in order to achieve the origin independence of the ROA invariants.

As examples, spectra for (R)-methyloxirane have been presented, which are related to the two-state approximation, which relates the Raman and ROA spectra at a single, electronically excited state, as well as its breakdown in a case where various electronic excitations play a role. Moreover, the calculation of the full Raman and ROA excitation profiles highlights the fact that in RT-TDDFT the whole frequency range is obtained in one go via Fourier transforms. Additionally, RT-TDDFT works well for a high density of states and shows a favorable scaling compared to LR-TDDFT. The presented technique allows for an origin independent calculation of ROA spectra and paves the way for the application to large systems, making use of both nonlocal pseudopotentials and the advantages of RT-TDDFT. In addition, it offers a promising way for the combination with *ab initio* molecular dynamics simulations for the inclusion of dynamic and environmental effects and modeling of the condensed phase.

ACKNOWLEDGMENTS

This work was supported by the University of Zurich, the University Research Priority Program "Solar Light to Chemical Energy Conversion" (LightChEC), and the Swiss National Science Foundation (Grant No. PP00P2_170667). Our calculations have been supported by the Swiss National Supercomputing Center (Account Nos. s745, s788, and s875).

APPENDIX A: REPRESENTATIONS

For a Hamiltonian of the form

$$\hat{H}_0 = \frac{\hat{p}^2}{2m_e} + \hat{V}^{\mathrm{loc}} + \hat{V}^{\mathrm{nl}}, \tag{A1}$$

where $\hat{V}^{\mathrm{loc}}$ groups all the local potentials and $\hat{V}^{\mathrm{nl}}$ stands for nonlocal potentials, e.g., for the nonlocal part of pseudopotentials, different representations of the linear response functions are derived, using the propagator formalism presented, e.g., in Ref. 95.

1. Electric-dipole–electric-dipole linear response

According to Eqs. (30)–(33), the mixed representation of $\alpha_{\alpha\beta}(\omega)$ can be obtained as

$$\begin{aligned}\hbar\omega\langle\langle\hat{r}_\alpha;\hat{r}_\beta\rangle\rangle_\omega &= \left\langle\left\langle\frac{i\hbar}{m_e}\hat{p}_\alpha + [\hat{r}_\alpha,\hat{V}^{\mathrm{nl}}];\hat{r}_\beta\right\rangle\right\rangle_\omega \\ &= \frac{i\hbar}{m_e}\langle\langle\hat{p}^{\mathrm{gen}}_\alpha;\hat{r}_\beta\rangle\rangle_\omega \\ &= -\frac{i\hbar}{m_e}\langle\langle\hat{r}_\alpha;\hat{p}^{\mathrm{gen}}_\beta\rangle\rangle_\omega,\end{aligned} \tag{A2}$$

and the velocity representation is derived by the means of

$$\begin{aligned}\hbar^2\omega^2\langle\langle\hat{r}_\alpha;\hat{r}_\beta\rangle\rangle_\omega &= \left\langle\frac{\hbar^2}{m_e}\delta_{\alpha\beta} + [[\hat{r}_\alpha,\hat{V}^{\mathrm{nl}}],\hat{r}_\beta]\right\rangle_0 \\ &\quad + \left\langle\left\langle\frac{i\hbar}{m_e}\hat{p}_\alpha + [\hat{r}_\alpha,\hat{V}^{\mathrm{nl}}];-\frac{i\hbar}{m_e}\hat{p}_\beta - [\hat{r}_\beta,\hat{V}^{\mathrm{nl}}]\right\rangle\right\rangle_\omega \\ &= \left\langle\frac{\hbar^2}{m_e}\delta_{\alpha\beta} + [[\hat{r}_\alpha,\hat{V}^{\mathrm{nl}}],\hat{r}_\beta]\right\rangle_0 + \frac{\hbar^2}{m_e^2}\langle\langle\hat{p}^{\mathrm{gen}}_\alpha;\hat{p}^{\mathrm{gen}}_\beta\rangle\rangle_\omega.\end{aligned} \tag{A3}$$

2. Electric-dipole–electric-quadrupole linear response

Similarly, there are two "mixed" representations of $A_{\alpha,\beta\gamma}(\omega)$,

$$\begin{aligned}\hbar\omega\langle\langle\hat{r}_\alpha;\hat{r}_\beta\hat{r}_\gamma\rangle\rangle_\omega &= \frac{i\hbar}{m_e}\langle\langle\hat{p}^{\mathrm{gen}}_\alpha;\hat{r}_\beta\hat{r}_\gamma\rangle\rangle_\omega \\ &= -\frac{i\hbar}{m_e}\left\langle\left\langle\hat{r}_\alpha;\hat{r}_\beta\hat{p}^{\mathrm{gen}}_\gamma + \hat{p}^{\mathrm{gen}}_\beta\hat{r}_\gamma\right\rangle\right\rangle_\omega\end{aligned} \tag{A4}$$

and a velocity representation using

$$\begin{aligned}\hbar^2\omega^2\langle\langle\hat{r}_\alpha;\hat{r}_\beta\hat{r}_\gamma\rangle\rangle_\omega &= -\frac{i\hbar}{m_e}\left\langle[\hat{r}_\alpha,(\hat{r}_\beta\hat{p}^{\mathrm{gen}}_\gamma + \hat{p}^{\mathrm{gen}}_\beta\hat{r}_\gamma)]\right\rangle_0 \\ &\quad + \frac{\hbar^2}{m_e^2}\left\langle\left\langle\hat{p}^{\mathrm{gen}}_\alpha;\hat{r}_\beta\hat{p}^{\mathrm{gen}}_\gamma + \hat{p}^{\mathrm{gen}}_\beta\hat{r}_\gamma\right\rangle\right\rangle_\omega \\ &= \frac{i\hbar}{m_e}\left\langle[\hat{p}^{\mathrm{gen}}_\alpha,\hat{r}_\beta\hat{r}_\gamma]\right\rangle_0 + \frac{\hbar^2}{m_e^2}\left\langle\left\langle\hat{p}^{\mathrm{gen}}_\alpha;\hat{r}_\beta\hat{p}^{\mathrm{gen}}_\gamma + \hat{p}^{\mathrm{gen}}_\beta\hat{r}_\gamma\right\rangle\right\rangle_\omega.\end{aligned} \tag{A5}$$

3. Electric-dipole–magnetic-dipole linear response

For $G_{\alpha\beta}(\omega)$, the length and velocity representations are related via

$$\begin{aligned}\hbar\omega\langle\langle\hat{r}_\alpha;\hat{m}^{\mathrm{gen}}_\beta\rangle\rangle_\omega &= \langle[\hat{r}_\alpha,\hat{m}^{\mathrm{gen}}_\beta]\rangle_0 + \langle\langle[\hat{r}_\alpha,\hat{H}_0];\hat{m}^{\mathrm{gen}}_\beta\rangle\rangle_\omega \\ &= \langle[\hat{r}_\alpha,\hat{m}^{\mathrm{gen}}_\beta]\rangle_0 + \frac{i\hbar}{m_e}\langle\langle\hat{p}^{\mathrm{gen}}_\alpha;\hat{m}^{\mathrm{gen}}_\beta\rangle\rangle_\omega.\end{aligned} \tag{A6}$$

APPENDIX B: ORIGIN DEPENDENCE OF INVARIANTS

In this section, we use atomic units.

The explicit origin dependence of $\boldsymbol{\alpha G}$ in a length representation of $G_{\alpha\beta}$ and $\alpha_{\alpha\beta}$ is

$$\begin{aligned}\alpha G^{O+a} &= \frac{1}{9}\mathrm{Im}\left\{\langle\langle\hat{r}^{O+a}_\alpha;\hat{r}^{O+a}_\alpha\rangle\rangle_\omega\langle\langle\hat{r}^{O+a}_\beta;\hat{m}^{\mathrm{gen},O+a}_\beta\rangle\rangle^*_\omega\right\} \\ &= \frac{1}{9}\mathrm{Im}\left\{\langle\langle\hat{r}^{O}_\alpha;\hat{r}^{O}_\alpha\rangle\rangle_\omega\left(\langle\langle\hat{r}^{O}_\beta;\hat{m}^{\mathrm{gen},O}_\beta\rangle\rangle_\omega + \frac{1}{2}\epsilon_{\beta\gamma\delta}a_\gamma\langle\langle\hat{r}^{O}_\beta;\hat{p}^{\mathrm{gen}}_\delta\rangle\rangle_\omega\right)^*\right\} \\ &= \alpha G^O + \frac{1}{18}\mathrm{Im}\left\{\langle\langle\hat{r}^{O}_\alpha;\hat{r}^{O}_\alpha\rangle\rangle_\omega\epsilon_{\beta\gamma\delta}a_\gamma\langle\langle\hat{r}^{O}_\beta;\hat{p}^{\mathrm{gen}}_\delta\rangle\rangle^*_\omega\right\} \\ &= \alpha G^O + \frac{1}{18}\mathrm{Im}\Big\{\langle\langle\hat{r}^{O}_\alpha;\hat{r}^{O}_\alpha\rangle\rangle_\omega\Big[a_y\langle\langle\hat{r}^{O}_x;\hat{p}^{\mathrm{gen}}_z\rangle\rangle^*_\omega - a_z\langle\langle\hat{r}^{O}_x;\hat{p}^{\mathrm{gen}}_y\rangle\rangle^*_\omega \\ &\quad + a_z\langle\langle\hat{r}^{O}_y;\hat{p}^{\mathrm{gen}}_x\rangle\rangle^*_\omega - a_x\langle\langle\hat{r}^{O}_y;\hat{p}^{\mathrm{gen}}_z\rangle\rangle^*_\omega + a_x\langle\langle\hat{r}^{O}_z;\hat{p}^{\mathrm{gen}}_y\rangle\rangle^*_\omega \\ &\quad - a_y\langle\langle\hat{r}^{O}_z;\hat{p}^{\mathrm{gen}}_x\rangle\rangle^*_\omega\Big]\Big\}.\end{aligned} \tag{B1}$$

A condition for the remaining term to vanish is

$$\langle\langle\hat{r}^{O}_\beta;\hat{p}^{\mathrm{gen}}_\alpha\rangle\rangle^*_\omega = \langle\langle\hat{r}^{O}_\alpha;\hat{p}^{\mathrm{gen}}_\beta\rangle\rangle^*_\omega. \tag{B2}$$

If we choose the velocity representation for $G_{\alpha\beta}$, the invariant contains the following terms:

$$\begin{aligned}\mathrm{Im}\Big\{\langle\langle\hat{r}_\alpha^{O+a};\hat{r}_\alpha^{O+a}\rangle\rangle_\omega\langle\langle\hat{p}_\beta^{\mathrm{gen}};\hat{m}_\beta^{\mathrm{gen},O+a}\rangle\rangle_\omega^*\Big\} &= \mathrm{Im}\Big\{\langle\langle\hat{r}_\alpha^{O};\hat{r}_\alpha^{O}\rangle\rangle_\omega\Big(\langle\langle\hat{p}_\beta^{\mathrm{gen}};\hat{m}_\beta^{\mathrm{gen},O}\rangle\rangle_\omega+\frac{1}{2}\epsilon_{\beta\gamma\delta}a_\gamma\langle\langle\hat{p}_\beta^{\mathrm{gen}};\hat{p}_\delta^{\mathrm{gen}}\rangle\rangle_\omega\Big)^*\Big\}\\ &= \langle\langle\hat{r}_\alpha^{O};\hat{r}_\alpha^{O}\rangle\rangle_\omega\langle\langle\hat{p}_\beta^{\mathrm{gen}};\hat{m}_\beta^{\mathrm{gen},O}\rangle\rangle_\omega^*+\frac{1}{2}\mathrm{Im}\Big\{\langle\langle\hat{r}_\alpha^{O};\hat{r}_\alpha^{O}\rangle\rangle_\omega\epsilon_{\beta\gamma\delta}a_\gamma\langle\langle\hat{p}_\beta^{\mathrm{gen}};\hat{p}_\delta^{\mathrm{gen}}\rangle\rangle_\omega^*\Big\}\\ &= \langle\langle\hat{r}_\alpha^{O};\hat{r}_\alpha^{O}\rangle\rangle_\omega\langle\langle\hat{p}_\beta^{\mathrm{gen}};\hat{m}_\beta^{\mathrm{gen},O}\rangle\rangle_\omega^*+\frac{1}{2}\mathrm{Im}\Big\{\langle\langle\hat{r}_\alpha^{O};\hat{r}_\alpha^{O}\rangle\rangle_\omega\Big[a_y\langle\langle\hat{p}_x^{\mathrm{gen}};\hat{p}_z^{\mathrm{gen}}\rangle\rangle_\omega^*-a_z\langle\langle\hat{p}_x^{\mathrm{gen}};\hat{p}_y^{\mathrm{gen}}\rangle\rangle_\omega^*\\ &\quad+a_z\langle\langle\hat{p}_y^{\mathrm{gen}};\hat{p}_x^{\mathrm{gen}}\rangle\rangle_\omega^*-a_x\langle\langle\hat{p}_y^{\mathrm{gen}};\hat{p}_z^{\mathrm{gen}}\rangle\rangle_\omega^*+a_x\langle\langle\hat{p}_z^{\mathrm{gen}};\hat{p}_y^{\mathrm{gen}}\rangle\rangle_\omega^*-a_y\langle\langle\hat{p}_z^{\mathrm{gen}};\hat{p}_x^{\mathrm{gen}}\rangle\rangle_\omega^*\Big]\Big\}.\end{aligned}\tag{B3}$$

In contrast to Eq. (B1), the additional terms in Eq. (B3) vanish for a finite basis set since the condition in Eq. (47) is fulfilled for $\hat{A}=\hat{B}=\hat{p}^{\mathrm{gen}}$. Note that, for $\boldsymbol{\alpha G}$, the representation for $\alpha_{\alpha\beta}$ can be chosen arbitrarily.

The origin dependence of $\beta(\boldsymbol{G})^2$ in a length representation of $G_{\alpha\beta}$ and $\alpha_{\alpha\beta}$ is

$$\begin{aligned}\beta^{O+a}(G)^2 &= \frac{1}{2}\mathrm{Im}\Big\{3\langle\langle\hat{r}_\alpha^{O+a};\hat{r}_\beta^{O+a}\rangle\rangle_\omega\langle\langle\hat{r}_\alpha^{O+a};\hat{m}_\beta^{\mathrm{gen},O+a}\rangle\rangle_\omega^*-\langle\langle\hat{r}_\alpha^{O+a};\hat{r}_\alpha^{O+a}\rangle\rangle_\omega\langle\langle\hat{r}_\beta^{O+a};\hat{m}_\beta^{\mathrm{gen},O+a}\rangle\rangle_\omega^*\Big\}\\ &= \frac{1}{2}\mathrm{Im}\Big\{3\langle\langle\hat{r}_\alpha^{O};\hat{r}_\beta^{O}\rangle\rangle_\omega\Big(\langle\langle\hat{r}_\alpha^{O};\hat{m}_\beta^{\mathrm{gen},O}\rangle\rangle_\omega+\frac{1}{2}\epsilon_{\beta\gamma\delta}a_\gamma\langle\langle\hat{r}_\alpha^{O};\hat{p}_\delta^{\mathrm{gen}}\rangle\rangle_\omega\Big)^*-\langle\langle\hat{r}_\alpha^{O};\hat{r}_\alpha^{O}\rangle\rangle_\omega\Big(\langle\langle\hat{r}_\beta^{O};\hat{m}_\beta^{\mathrm{gen},O}\rangle\rangle_\omega+\frac{1}{2}\epsilon_{\beta\gamma\delta}a_\gamma\langle\langle\hat{r}_\beta^{O};\hat{p}_\delta^{\mathrm{gen}}\rangle\rangle_\omega\Big)^*\Big\}\\ &= \beta^{O}(G)^2+\frac{1}{4}\mathrm{Im}\Big\{3\langle\langle\hat{r}_\alpha^{O};\hat{r}_\beta^{O}\rangle\rangle_\omega\epsilon_{\beta\gamma\delta}a_\gamma\langle\langle\hat{r}_\alpha^{O};\hat{p}_\delta^{\mathrm{gen}}\rangle\rangle_\omega^*-\langle\langle\hat{r}_\alpha^{O};\hat{r}_\alpha^{O}\rangle\rangle_\omega\epsilon_{\beta\gamma\delta}a_\gamma\langle\langle\hat{r}_\beta^{O};\hat{p}_\delta^{\mathrm{gen}}\rangle\rangle_\omega^*\Big\},\end{aligned}\tag{B4}$$

where the last summand does not vanish for a finite basis set. If we choose the velocity representation for $G_{\alpha\beta}$, the invariant contains terms of the following form:

$$\begin{aligned}&\mathrm{Im}\Big\{3\langle\langle\hat{r}_\alpha^{O+a};\hat{r}_\beta^{O+a}\rangle\rangle_\omega\langle\langle\hat{p}_\alpha^{\mathrm{gen},O+a};\hat{m}_\beta^{\mathrm{gen},O+a}\rangle\rangle_\omega^*-\langle\langle\hat{r}_\alpha^{O+a};\hat{r}_\alpha^{O+a}\rangle\rangle_\omega\langle\langle\hat{p}_\beta^{\mathrm{gen},O+a};\hat{m}_\beta^{\mathrm{gen},O+a}\rangle\rangle_\omega^*\Big\}\\ &= \mathrm{Im}\Big\{3\langle\langle\hat{r}_\alpha^{O};\hat{r}_\beta^{O}\rangle\rangle_\omega\Big(\langle\langle\hat{p}_\alpha^{\mathrm{gen},O};\hat{m}_\beta^{\mathrm{gen},O}\rangle\rangle_\omega+\frac{1}{2}\epsilon_{\beta\gamma\delta}a_\gamma\langle\langle\hat{p}_\alpha^{\mathrm{gen},O};\hat{p}_\delta^{\mathrm{gen}}\rangle\rangle_\omega\Big)^*\\ &\quad-\langle\langle\hat{r}_\alpha^{O};\hat{r}_\alpha^{O}\rangle\rangle_\omega\Big(\langle\langle\hat{p}_\beta^{\mathrm{gen},O};\hat{m}_\beta^{\mathrm{gen},O}\rangle\rangle_\omega+\frac{1}{2}\epsilon_{\beta\gamma\delta}a_\gamma\langle\langle\hat{p}_\beta^{\mathrm{gen},O};\hat{p}_\delta^{\mathrm{gen}}\rangle\rangle_\omega\Big)^*\Big\}\\ &= \mathrm{Im}\Big\{3\langle\langle\hat{r}_\alpha^{O};\hat{r}_\beta^{O}\rangle\rangle_\omega\langle\langle\hat{p}_\alpha^{\mathrm{gen}};\hat{m}_\beta^{\mathrm{gen}}\rangle\rangle_\omega^*-\langle\langle\hat{r}_\alpha^{O};\hat{r}_\alpha^{O}\rangle\rangle_\omega\langle\langle\hat{p}_\beta^{\mathrm{gen}};\hat{m}_\beta^{\mathrm{gen}}\rangle\rangle_\omega^*\Big\}\\ &\quad+\frac{1}{2}\mathrm{Im}\Big\{3\langle\langle\hat{r}_\alpha^{O};\hat{r}_\beta^{O}\rangle\rangle_\omega\epsilon_{\beta\gamma\delta}a_\gamma\langle\langle\hat{p}_\alpha^{\mathrm{gen}};\hat{p}_\delta^{\mathrm{gen}}\rangle\rangle_\omega^*-\langle\langle\hat{r}_\alpha^{O};\hat{r}_\alpha^{O}\rangle\rangle_\omega\epsilon_{\beta\gamma\delta}a_\gamma\langle\langle\hat{p}_\beta^{\mathrm{gen}};\hat{p}_\delta^{\mathrm{gen}}\rangle\rangle_\omega^*\Big\},\end{aligned}\tag{B5}$$

where again the last summand would have to vanish for a finite basis set, in order to get an origin independent result. Note that the very last term is the same as in Eq. (B3) and consequently the same argumentation applies. However, the first term in the last summand is more involved and reads

$$\begin{aligned}3\langle\langle\hat{r}_\alpha^{O};\hat{r}_\beta^{O}\rangle\rangle_\omega\epsilon_{\beta\gamma\delta}a_\gamma\langle\langle\hat{p}_\alpha^{\mathrm{gen}}\hat{p}_\delta^{\mathrm{gen}}\rangle\rangle_\omega^* &= 3\langle\langle\hat{r}_x^{O};\hat{r}_x^{O}\rangle\rangle_\omega\Big(a_y\langle\langle\hat{p}_x^{\mathrm{gen}};\hat{p}_z^{\mathrm{gen}}\rangle\rangle_\omega^*-a_z\langle\langle\hat{p}_x^{\mathrm{gen}};\hat{p}_y^{\mathrm{gen}}\rangle\rangle_\omega^*\Big)+3\langle\langle\hat{r}_x^{O};\hat{r}_y^{O}\rangle\rangle_\omega\Big(a_z\langle\langle\hat{p}_x^{\mathrm{gen}};\hat{p}_x^{\mathrm{gen}}\rangle\rangle_\omega^*-a_x\langle\langle\hat{p}_x^{\mathrm{gen}};\hat{p}_z^{\mathrm{gen}}\rangle\rangle_\omega^*\Big)\\ &\quad+3\langle\langle\hat{r}_x^{O};\hat{r}_z^{O}\rangle\rangle_\omega\Big(a_x\langle\langle\hat{p}_x^{\mathrm{gen}};\hat{p}_y^{\mathrm{gen}}\rangle\rangle_\omega^*-a_y\langle\langle\hat{p}_x^{\mathrm{gen}};\hat{p}_x^{\mathrm{gen}}\rangle\rangle_\omega^*\Big)+3\langle\langle\hat{r}_y^{O};\hat{r}_x^{O}\rangle\rangle_\omega\Big(a_y\langle\langle\hat{p}_y^{\mathrm{gen}};\hat{p}_z^{\mathrm{gen}}\rangle\rangle_\omega^*-a_z\langle\langle\hat{p}_y^{\mathrm{gen}};\hat{p}_y^{\mathrm{gen}}\rangle\rangle_\omega^*\Big)\\ &\quad+3\langle\langle\hat{r}_y^{O};\hat{r}_y^{O}\rangle\rangle_\omega\Big(a_z\langle\langle\hat{p}_y^{\mathrm{gen}};\hat{p}_x^{\mathrm{gen}}\rangle\rangle_\omega^*-a_x\langle\langle\hat{p}_y^{\mathrm{gen}};\hat{p}_z^{\mathrm{gen}}\rangle\rangle_\omega^*\Big)+3\langle\langle\hat{r}_y^{O};\hat{r}_z^{O}\rangle\rangle_\omega\Big(a_x\langle\langle\hat{p}_y^{\mathrm{gen}};\hat{p}_y^{\mathrm{gen}}\rangle\rangle_\omega^*-a_y\langle\langle\hat{p}_y^{\mathrm{gen}};\hat{p}_x^{\mathrm{gen}}\rangle\rangle_\omega^*\Big)\\ &\quad+3\langle\langle\hat{r}_z^{O};\hat{r}_x^{O}\rangle\rangle_\omega\Big(a_y\langle\langle\hat{p}_z^{\mathrm{gen}};\hat{p}_z^{\mathrm{gen}}\rangle\rangle_\omega^*-a_z\langle\langle\hat{p}_z^{\mathrm{gen}};\hat{p}_y^{\mathrm{gen}}\rangle\rangle_\omega^*\Big)+3\langle\langle\hat{r}_z^{O};\hat{r}_y^{O}\rangle\rangle_\omega\Big(a_z\langle\langle\hat{p}_z^{\mathrm{gen}};\hat{p}_x^{\mathrm{gen}}\rangle\rangle_\omega^*-a_x\langle\langle\hat{p}_z^{\mathrm{gen}};\hat{p}_z^{\mathrm{gen}}\rangle\rangle_\omega^*\Big)\\ &\quad+3\langle\langle\hat{r}_z^{O};\hat{r}_z^{O}\rangle\rangle_\omega\Big(a_x\langle\langle\hat{p}_z^{\mathrm{gen}};\hat{p}_y^{\mathrm{gen}}\rangle\rangle_\omega^*-a_y\langle\langle\hat{p}_z^{\mathrm{gen}};\hat{p}_x^{\mathrm{gen}}\rangle\rangle_\omega^*\Big).\end{aligned}\tag{B6}$$

Grouping the terms in the factors of a_α gives

$$\begin{aligned}3\langle\langle\hat{r}_\alpha^{O};\hat{r}_\beta^{O}\rangle\rangle_\omega\epsilon_{\beta\gamma\delta}a_\gamma\langle\langle\hat{p}_\alpha^{\mathrm{gen}};\hat{p}_\delta^{\mathrm{gen}}\rangle\rangle_\omega^* &= 3a_x\Big(\langle\langle\hat{r}_x^{O};\hat{r}_z^{O}\rangle\rangle_\omega\langle\langle\hat{p}_x^{\mathrm{gen}};\hat{p}_y^{\mathrm{gen}}\rangle\rangle_\omega^*+\langle\langle\hat{r}_y^{O};\hat{r}_z^{O}\rangle\rangle_\omega\langle\langle\hat{p}_y^{\mathrm{gen}};\hat{p}_y^{\mathrm{gen}}\rangle\rangle_\omega^*+\langle\langle\hat{r}_z^{O};\hat{r}_z^{O}\rangle\rangle_\omega\langle\langle\hat{p}_z^{\mathrm{gen}};\hat{p}_y^{\mathrm{gen}}\rangle\rangle_\omega^*\\ &\quad-\langle\langle\hat{r}_x^{O};\hat{r}_y^{O}\rangle\rangle_\omega\langle\langle\hat{p}_x^{\mathrm{gen}};\hat{p}_z^{\mathrm{gen}}\rangle\rangle_\omega^*-\langle\langle\hat{r}_y^{O};\hat{r}_y^{O}\rangle\rangle_\omega\langle\langle\hat{p}_y^{\mathrm{gen}};\hat{p}_z^{\mathrm{gen}}\rangle\rangle_\omega^*-\langle\langle\hat{r}_z^{O};\hat{r}_y^{O}\rangle\rangle_\omega\langle\langle\hat{p}_z^{\mathrm{gen}};\hat{p}_z^{\mathrm{gen}}\rangle\rangle_\omega^*\Big)\\ &\quad+3a_y\Big(\langle\langle\hat{r}_x^{O};\hat{r}_x^{O}\rangle\rangle_\omega\langle\langle\hat{p}_x^{\mathrm{gen}};\hat{p}_z^{\mathrm{gen}}\rangle\rangle_\omega^*+\langle\langle\hat{r}_y^{O};\hat{r}_x^{O}\rangle\rangle_\omega\langle\langle\hat{p}_y^{\mathrm{gen}};\hat{p}_z^{\mathrm{gen}}\rangle\rangle_\omega^*+\langle\langle\hat{r}_z^{O};\hat{r}_x^{O}\rangle\rangle_\omega\langle\langle\hat{p}_z^{\mathrm{gen}};\hat{p}_z^{\mathrm{gen}}\rangle\rangle_\omega^*\\ &\quad-\langle\langle\hat{r}_x^{O};\hat{r}_z^{O}\rangle\rangle_\omega\langle\langle\hat{p}_x^{\mathrm{gen}};\hat{p}_x^{\mathrm{gen}}\rangle\rangle_\omega^*-\langle\langle\hat{r}_y^{O};\hat{r}_z^{O}\rangle\rangle_\omega\langle\langle\hat{p}_y^{\mathrm{gen}};\hat{p}_x^{\mathrm{gen}}\rangle\rangle_\omega^*-\langle\langle\hat{r}_z^{O};\hat{r}_z^{O}\rangle\rangle_\omega\langle\langle\hat{p}_z^{\mathrm{gen}};\hat{p}_x^{\mathrm{gen}}\rangle\rangle_\omega^*\Big)\\ &\quad+3a_z\Big(\langle\langle\hat{r}_x^{O};\hat{r}_y^{O}\rangle\rangle_\omega\langle\langle\hat{p}_x^{\mathrm{gen}};\hat{p}_x^{\mathrm{gen}}\rangle\rangle_\omega^*+\langle\langle\hat{r}_y^{O};\hat{r}_y^{O}\rangle\rangle_\omega\langle\langle\hat{p}_y^{\mathrm{gen}};\hat{p}_x^{\mathrm{gen}}\rangle\rangle_\omega^*+\langle\langle\hat{r}_z^{O};\hat{r}_y^{O}\rangle\rangle_\omega\langle\langle\hat{p}_z^{\mathrm{gen}};\hat{p}_x^{\mathrm{gen}}\rangle\rangle_\omega^*\\ &\quad-\langle\langle\hat{r}_x^{O};\hat{r}_x^{O}\rangle\rangle_\omega\langle\langle\hat{p}_x^{\mathrm{gen}};\hat{p}_y^{\mathrm{gen}}\rangle\rangle_\omega^*-\langle\langle\hat{r}_y^{O};\hat{r}_x^{O}\rangle\rangle_\omega\langle\langle\hat{p}_y^{\mathrm{gen}};\hat{p}_y^{\mathrm{gen}}\rangle\rangle_\omega^*-\langle\langle\hat{r}_z^{O};\hat{r}_x^{O}\rangle\rangle_\omega\langle\langle\hat{p}_z^{\mathrm{gen}};\hat{p}_y^{\mathrm{gen}}\rangle\rangle_\omega^*\Big).\end{aligned}\tag{B7}$$

$\beta(A)^2$ can be expanded in a similar manner. Extending this for different representations leads to the condition in Eq. (48).

REFERENCES

[1] L. D. Barron, L. Hecht, I. H. McColl, and E. W. Blanch, Mol. Phys. **102**, 731 (2004).
[2] J. Costante, L. Hecht, P. L. Polavarapu, A. Collet, and L. D. Barron, Angew. Chem., Int. Ed. Engl. **36**, 885 (1997).
[3] E. W. Blanch, L. Hecht, L. A. Day, D. M. Pederson, and L. D. Barron, J. Am. Chem. Soc. **123**, 4863 (2001).
[4] P. Oulevey, S. Luber, B. Varnholt, and T. Bürgi, Angew. Chem., Int. Ed. **55**, 11787 (2016).
[5] I. H. McColl, E. W. Blanch, L. Hecht, N. R. Kallenbach, and L. D. Barron, J. Am. Chem. Soc. **126**, 5076 (2004).
[6] L. D. Barron, Biomed. Spectrosc. Imaging **4**, 223 (2015).
[7] J. Šebestík and P. Bouř, Angew. Chem., Int. Ed. **53**, 9236 (2014).
[8] J. Kapitán, L. D. Barron, and L. Hecht, J. Raman Spectrosc. **46**, 392 (2015).
[9] P. Atkins and L. Barron, Mol. Phys. **16**, 453 (1969).
[10] L. Barron and A. Buckingham, Mol. Phys. **20**, 1111 (1971).
[11] L. Barron and A. Buckingham, Annu. Rev. Phys. Chem. **26**, 381 (1975).
[12] L. Hecht, L. Barron, and W. Hug, Chem. Phys. Lett. **158**, 341 (1989).
[13] W. Hug and H. Surbeck, Chem. Phys. Lett. **60**, 186 (1979).
[14] P. Bose, L. Barron, and P. Polavarapu, Chem. Phys. Lett. **155**, 423 (1989).
[15] M. Pecul, A. Rizzo, and J. Leszczynski, J. Phys. Chem. A **106**, 11008 (2002).
[16] E. Lamparska, V. Liégeois, O. Quinet, and B. Champagne, ChemPhysChem **7**, 2366 (2006).
[17] M. Reiher, V. Liégeois, and K. Ruud, J. Phys. Chem. A **109**, 7567 (2005).
[18] V. Liégeois, O. Quinet, and B. Champagne, J. Chem. Phys. **122**, 214304 (2005).
[19] S. Luber and M. Reiher, J. Phys. Chem. B **114**, 1057 (2010).
[20] C. Jacob, S. Luber, and M. Reiher, Chem. - Eur. J. **15**, 13491 (2009).
[21] X. Drooghaag, J. Marchand-Brynaert, B. Champagne, and V. Liégeois, J. Phys. Chem. B **114**, 11753 (2010).
[22] S. Yamamoto, Anal. Bioanal. Chem. **403**, 2203 (2012).
[23] J. Kessler, J. Kapitán, and P. Bouř, J. Phys. Chem. Lett. **6**, 3314 (2015).
[24] J. Bloino, M. Biczysko, and V. Barone, J. Phys. Chem. A **119**, 11862 (2015).
[25] T. D. Crawford and K. Ruud, ChemPhysChem **12**, 3442 (2011).
[26] M. Pecul and A. Rizzo, Mol. Phys. **101**, 2073 (2003).
[27] V. Liégeois, K. Ruud, and B. Champagne, J. Chem. Phys. **127**, 204105 (2007).
[28] S. Luber and M. Reiher, Chem. Phys. **346**, 212 (2008).
[29] P. Bouř, V. Baumruk, and J. Hanzliková, Collect. Czech. Chem. Commun. **62**, 1384 (1997).
[30] K. V. J. Jovan and K. Raghavachari, J. Chem. Theory Comput. **12**, 585 (2016).
[31] S. Luber and M. Reiher, ChemPhysChem **10**, 2049 (2009).
[32] S. Luber, J. Chem. Theory Comput. **13**, 1254 (2017).
[33] M. Pecul, E. Lamparska, C. Cappelli, L. Frediani, and K. Ruud, J. Phys. Chem. A **110**, 2807 (2006).
[34] S. Luber, J. Phys. Chem. A **117**, 2760 (2013).
[35] F. Egidi, V. Barone, J. Bloino, and C. Cappelli, J. Chem. Theory Comput. **8**, 585 (2012).
[36] F. Santoro, C. Cappelli, and V. Barone, J. Chem. Theory Comput. **7**, 1824 (2011).
[37] T. Giovannini, G. Del Frate, P. Lafiosca, and C. Cappelli, Phys. Chem. Chem. Phys. **20**, 9181 (2018).
[38] J. R. Cheeseman, M. S. Shaik, P. L. Popelier, and E. W. Blanch, J. Am. Chem. Soc. **133**, 4991 (2011).
[39] S. Yamamoto, J. Kaminský, and P. Bouř, Anal. Chem. **84**, 2440 (2012).
[40] K. H. Hopmann, K. Ruud, M. Pecul, A. Kudelski, M. Dracínský, and P. Bour, J. Phys. Chem. B **115**, 4128 (2011).
[41] F. Lipparini, F. Egidi, C. Cappelli, and V. Barone, J. Chem. Theory Comput. **9**, 1880 (2013).
[42] T. Giovannini, M. Olszówka, F. Egidi, J. R. Cheeseman, G. Scalmani, and C. Cappelli, J. Chem. Theory Comput. **13**, 4421 (2017).
[43] S. Luber and M. Reiher, ChemPhysChem **11**, 1876 (2010).
[44] C. Johannessen, L. Hecht, and C. Merten, ChemPhysChem **12**, 1419 (2011).
[45] M. Humbert-Droz, P. Oulevey, L. M. Lawson Daku, S. Luber, H. Hagemann, and T. Bürgi, Phys. Chem. Chem. Phys. **16**, 23260 (2014).
[46] S. Luber, Biomed. Spectrosc. Imaging **4**, 255 (2015).
[47] M. Pecul and K. Ruud, Int. J. Quantum Chem. **104**, 816 (2005).
[48] T. D. Crawford, Theor. Chem. Acc. **115**, 227 (2006).
[49] K. Ruud and A. J. Thorvaldsen, Chirality **21**, E54 (2009).
[50] S. T. Mutter, F. Zielinski, P. L. Popelier, and E. W. Blanch, Analyst **140**, 2944 (2015).
[51] A. C. Albrecht, J. Chem. Phys. **34**, 1476 (1961); e-print arXiv:9809069v1 [arXiv:gr-qc].
[52] A. Warshel and P. Dauber, J. Chem. Phys. **66**, 5477 (1977).
[53] S. Lee and E. J. Heller, J. Chem. Phys. **71**, 4777 (1979).
[54] E. J. Heller, R. L. Sundberg, and D. Tannor, J. Phys. Chem. **86**, 1822 (1982).
[55] D. J. Tannor and E. J. Heller, J. Chem. Phys. **77**, 202 (1982); e-print arXiv:9809069v1 [arXiv:gr-qc].
[56] S. Luber, J. Neugebauer, and M. Reiher, J. Chem. Phys. **132**, 044113 (2010).
[57] L. N. Vidal, F. Egidi, V. Barone, and C. Cappelli, J. Chem. Phys. **142**, 174101 (2015).
[58] L. N. Vidal, T. Giovannini, and C. Cappelli, J. Phys. Chem. Lett. **7**, 3585 (2016).
[59] A. Baiardi, J. Bloino, and V. Barone, J. Chem. Theory Comput. **14**, 6370 (2018).
[60] L. Jensen, J. Autschbach, M. Krykunov, and G. C. Schatz, J. Chem. Phys. **127**, 134101 (2007).
[61] F. Krausbeck, J. Autschbach, and M. Reiher, J. Phys. Chem. A **120**, 9740 (2016).
[62] J. R. Rouxel, Y. Zhang, and S. Mukamel, Chem. Sci. **10**, 898 (2019).
[63] M. A. L. Marques and A. Rubio, in *Time-Dependent Density Functional Theory*, edited by M. Marques, C. A. Ullrich, F. Nogueira, A. Rubio, K. Burke, and E. K. Gross (Springer-Verlag Berlin Heidelberg, 2006), Chap. 15, pp. 227–240.
[64] A. Bruner, D. LaMaster, and K. Lopata, J. Chem. Theory Comput. **12**, 3741 (2016).
[65] J. Mattiat and S. Luber, J. Chem. Phys. **149**, 174108 (2018).
[66] D. R. Hamann, M. Schlüter, and C. Chiang, Phys. Rev. Lett. **43**, 1494 (1979).
[67] L. Kleinman and D. M. Bylander, Phys. Rev. Lett. **48**, 1425 (1982).
[68] CP2K Version 7.0 (Developement Version), the Cp2k Developers Group, 2019; available from http://www.cp2k.org.
[69] J. Vandevondele, M. Krack, F. Mohamed, M. Parrinello, T. Chassaing, and J. Hutter, Comput. Phys. Commun. **167**, 103 (2005).
[70] J. Hutter, M. Iannuzzi, F. Schiffmann, and J. Vandevondele, Wiley Interdiscip. Rev.: Comput. Mol. Sci. **4**, 15 (2014); e-print arXiv:9512004 [mtrl-th].
[71] S. Luber, Phys. Chem. Chem. Phys. **20**, 28751 (2018).
[72] T. Helgaker, K. Ruud, K. L. Bak, P. Jørgensen, and J. Olsen, Faraday Discuss. **99**, 165 (1994).
[73] F. London, J. Phys. Radium **8**, 397 (1937).
[74] K. L. Bak, A. E. Hansen, K. Ruud, T. Helgaker, J. Olsen, and P. Jørgensen, Theor. Chim. Acta **90**, 441 (1995).
[75] A. M. Lee, N. C. Handy, and S. M. Colwell, J. Chem. Phys. **103**, 10095 (1995).
[76] M. Pecul, K. Ruud, and T. Helgaker, Chem. Phys. Lett. **388**, 110 (2004).
[77] K. Ruud, T. Helgaker, and P. Bour, J. Chem. Phys. A **106**, 7448 (2002).
[78] T. B. Pedersen, H. Koch, L. Boman, and A. M. S. de Merás, Chem. Phys. Lett. **393**, 319 (2004).
[79] C. J. Pickard and F. Mauri, Phys. Rev. B **63**, 245101 (2001); e-print arXiv:0101257 [cond-mat].
[80] C. J. Pickard and F. Mauri, Phys. Rev. Lett. **91**, 196401 (2003); e-print arXiv:0304115 [cond-mat].
[81] S. Ismail-Beigi, E. K. Chang, and S. G. Louie, Phys. Rev. Lett. **87**, 087402 (2001); e-print arXiv:0101383 [cond-mat].
[82] J. Mattiat and S. Luber, Chem. Phys. **527**, 110464 (2019).
[83] D. Varsano, L. A. Espinosa-Leal, X. Andrade, M. A. L. Marques, R. di Felice, and A. Rubio, Phys. Chem. Chem. Phys. **11**, 4481 (2009).

[84]A. D. Buckingham, "Permanent and induced molecular moments and long-range intermolecular forces," in *Advances in Chemical Physics* (John Wiley & Sons, Ltd., 1967), pp. 107–142.
[85]L. D. Barron, *Molecular Light Scattering and Optical Activity*, 2nd ed. (Cambridge University Press, Cambridge, 2004).
[86]L. A. Nafie, Theor. Chem. Acc. **119**, 39 (2008).
[87]L. Hecht and L. A. Nafie, Mol. Phys. **72**, 441 (1991).
[88]D. J. Tannor, *Introduction to Quantum Mechanics: A Time-Dependent Perspective* (University Science Books, Mill Valley, CA, 2007).
[89]S. Lee, J. Chem. Phys. **78**, 723 (1983).
[90]L. Jensen, L. L. Zhao, J. Autschbach, and G. C. Schatz, J. Chem. Phys. **123**, 174110 (2005).
[91]G. Placzek, Z. Phys. **70**, 84 (1931).
[92]K. A. Kane and L. Jensen, J. Chem. Phys. C **114**, 5540 (2010).
[93]M. Thomas, F. Latorre, and P. Marquetand, J. Chem. Phys. **138**, 044101 (2013).
[94]J. Neugebauer, M. Reiher, C. Kind, and B. A. Hess, J. Comput. Chem. **23**, 895 (2002).
[95]J. Linderberg and Y. Öhrn, *Propagators in Quantum Chemistry* (John Wiley & Sons, 2004).
[96]J. Jensen and A. R. Mackintosh, *Rare Earth Magnetism: Structures and Excitations* (Clarendon Press, Oxford, 1991), pp. 134–162.
[97]R. Kubo, J. Phys. Soc. Jpn. Part 1 **12**, 570 (1957).
[98]T. B. Pedersen, H. Koch, and K. Ruud, J. Chem. Phys. **110**, 2883 (1999).
[99]D. H. Kobe and K.-H. Yang, Phys. Rev. A **32**, 952 (1985).
[100]L. Boßmann, R. Grummt, and M. Kolb, Lett. Math. Phys. **108**, 185 (2018).
[101]A. E. Hansen, Theor. Chim. Acta **16**, 217 (1970).
[102]T. B. Pedersen and A. E. Hansen, Chem. Phys. Lett. **246**, 1 (1995).
[103]F. Ding, W. Liang, C. T. Chapman, C. M. Isborn, and X. Li, J. Chem. Phys. **135**, 164101 (2011).
[104]F. Furche, J. Chem. Phys. **114**, 5982 (2001).
[105]M. Krykunov and J. Autschbach, J. Chem. Phys. **125**, 034102 (2006).
[106]M. Krykunov and J. Autschbach, J. Chem. Phys. **126**, 024101 (2007).
[107]T. B. Pedersen and H. Koch, J. Chem. Phys. **106**, 8059 (1997).
[108]S. Andermatt, J. Cha, F. Schiffmann, and J. VandeVondele, J. Chem. Theory Comput. **12**, 3214 (2016).
[109]K. Yabana, T. Nakatsukasa, J.-I. Iwata, and G. F. Bertsch, Phys. Status Solidi B **243**, 1121 (2006).
[110]J. P. Perdew, K. Burke, and M. Ernzerhof, Phys. Rev. Lett. **77**, 3865 (1996).
[111]J. VandeVondele and J. Hutter, J. Chem. Phys. **127**, 114105 (2007).
[112]S. Goedecker, M. Teter, and J. Hutter, Phys. Rev. B **54**, 1703 (1996).
[113]M. Carnell, S. Peyerimhoff, A. Breest, K. Gödderz, P. Ochmann, and J. Hormes, Chem. Phys. Lett. **180**, 477 (1991).
[114]D. Cohen, M. Levi, H. Basch, and A. Gedanken, J. Am. Chem. Soc. **105**, 1738 (1983).
[115]J. Šebestík and P. Bouř, J. Phys. Chem. Lett. **2**, 498 (2011).
[116]L. A. Nafie, Chem. Phys. **205**, 309 (1996).
[117]S. Tussupbayev, N. Govind, K. Lopata, and C. J. Cramer, J. Chem. Theory Comput. **11**, 1102 (2015).